

## Future projections of wind energy potentials in the arctic for the 21st century under the RCP8.5 scenario from regional climate models (Arctic-CORDEX)

Mirseid Akperov<sup>a,\*</sup>, Alexey V. Eliseev<sup>a,c,p</sup>, Annette Rinke<sup>b</sup>, Igor I. Mokhov<sup>a,c</sup>, Vladimir A. Semenov<sup>a,d</sup>, Mariya Dembitskaya<sup>a</sup>, Heidrun Matthes<sup>b</sup>, Muralidhar Adakudlu<sup>q</sup>, Fredrik Boberg<sup>n</sup>, Jens H. Christensen<sup>e,f,n</sup>, Klaus Dethloff<sup>b</sup>, Xavier Fettweis<sup>g</sup>, Oliver Gutjahr<sup>h</sup>, Günther Heinemann<sup>i</sup>, Torben Koenigk<sup>j,k</sup>, Dmitry Sein<sup>l,r</sup>, René Laprise<sup>m</sup>, Ruth Mottram<sup>n</sup>, Oumarou Nikiéma<sup>m</sup>, Stefan Sobolowski<sup>e</sup>, Katja Winger<sup>m</sup>, Wenxin Zhang<sup>o</sup>

<sup>a</sup> A.M. Obukhov Institute of Atmospheric Physics, RAS, Moscow, Russia

<sup>b</sup> Alfred Wegener Institute, Helmholtz Centre for Polar and Marine Research, AWI, Potsdam, Germany

<sup>c</sup> Lomonosov Moscow State University, Moscow, Russia

<sup>d</sup> Institute of Geography, RAS, Moscow, Russia

<sup>e</sup> NORCE Norwegian Research Centre, Bjerknes Centre for Climate Research, Bergen, Norway

<sup>f</sup> University of Copenhagen, Niels Bohr Institute, Denmark

<sup>g</sup> Department of Geography, University of Liège, Belgium

<sup>h</sup> Max Planck Institute for Meteorology, Hamburg, Germany

<sup>i</sup> Environmental Meteorology, Faculty of Regional and Environmental Sciences, University of Trier, Germany

<sup>j</sup> Swedish Meteorological and Hydrological Institute, Norrköping, Sweden

<sup>k</sup> Bolin Centre for Climate Research, Stockholm University, Stockholm, Sweden

<sup>l</sup> Alfred Wegener Institute, Helmholtz Centre for Polar and Marine Research, AWI, Bremerhaven, Germany

<sup>m</sup> Centre ESCER, Université du Québec à Montréal, Montréal, Québec, Canada

<sup>n</sup> Danish Meteorological Institute, Copenhagen, Denmark

<sup>o</sup> Department of Physical Geography and Ecosystem Science, Lund University, 22362 Lund, Sweden

<sup>p</sup> Institute of Applied Physics, Russian Academy of Sciences, Nizhny Novgorod, Russia

<sup>q</sup> Norwegian Meteorological Institute, Oslo, Norway

<sup>r</sup> Shirshov Institute of Oceanology, Russian Academy of Sciences, Moscow, Russia

### ARTICLE INFO

#### Keywords:

Arctic  
Wind speed  
Wind energy  
Climate change  
Sea ice  
Biogeophysical feedback  
Surface roughness  
Regional climate models  
ERAS  
CORDEX

### ABSTRACT

The Arctic has warmed more than twice the rate of the entire globe. To quantify possible climate change effects, we calculate wind energy potentials from a multi-model ensemble of Arctic-CORDEX. For this, we analyze future changes of wind power density (WPD) using an eleven-member multi-model ensemble. Impacts are estimated for two periods (2020–2049 and 2070–2099) of the 21st century under a high emission scenario (RCP8.5). The multi-model mean reveals an increase of seasonal WPD over the Arctic in the future decades. WPD variability across a range of temporal scales is projected to increase over the Arctic. The signal amplifies by the end of 21st century. Future changes in the frequency of wind speeds at 100 m not useable for wind energy production (wind speeds below 4 m/s or above 25 m/s) has been analyzed. The RCM ensemble simulates a more frequent occurrence of 100 m non-usable wind speeds for the wind-turbines over Scandinavia and selected land areas in Alaska, northern Russia and Canada. In contrast, non-usable wind speeds decrease over large parts of Eastern Siberia and in northern Alaska. Thus, our results indicate increased potential of the Arctic for the development and production of wind energy. Bias corrected and not corrected near-surface wind speed and WPD changes have been compared with each other. It has been found that both show the same sign of future change, but differ in magnitude of these changes. The role of sea-ice retreat and vegetation expansion in the Arctic in future on near-surface wind speed variability has been also assessed. Surface roughness through sea-ice and vegetation changes may significantly impact on WPD variability in the Arctic.

\* Corresponding author.

E-mail address: [aseid@ifaran.ru](mailto:aseid@ifaran.ru) (M. Akperov).

<https://doi.org/10.1016/j.ancene.2023.100402>

Received 21 September 2022; Received in revised form 17 July 2023; Accepted 23 July 2023

Available online 13 September 2023

2213-3054/© 2023 Elsevier Ltd. All rights reserved.

## 1. Introduction

The Arctic warming in recent decades has proceeded at approximate twice the rate of the global mean temperature increase – locally more than four times the global rate - and is accompanied by the unprecedented during the instrumental period reduction of sea ice extent (Jansen et al., 2020; Rantanen et al., 2022). Retreating sea ice amplifies warming, which in turn feeds back to further enhanced changes in the Arctic Ocean (Vihma, 2014; Semenov and Latif, 2015; Mokhov and Parfenova, 2021). Retreating sea ice already allows better access by sea to the Arctic Ocean, which can be seen for marine shipping along the Northern Sea Route (Khon et al., 2017; Kibanova et al., 2018; Parfenova et al., 2021), may ease the extraction of oil and natural gas resources and increase the opportunities for renewable energy production in the Arctic off-shore zones.

As the Arctic is a remote area, the energy supply of the Arctic regions is based on autonomous energy sources, mainly diesel power plants/generators and thermal power plants. Despite the high cost of electricity generated by these plants, they are also sources of greenhouse gas emissions. Using renewable energy to power the Arctic can be a cost-effective solution. Wind farms and related infrastructure are currently being built in the Arctic. Pilot projects are underway in Canada, Russia, Greenland and the USA to convert remote villages from diesel to hybrid wind and solar power (Krylytsov and Solovov, 2019; Akperov et al., 2022).

Investigating the spatial and temporal variability of near-surface wind speed is critical to assess the current wind energy potential and evaluate its future changes as the world continues to warm (Pryor et al., 2005; Moemken et al., 2018). The local near-surface wind speed variability is determined by large-scale, synoptic, and meso-scale circulations (storms, polar lows) as well as local conditions (Jakobson et al., 2019; Fabiano et al., 2020; Heinemann et al., 2022; Rapella et al., 2023). Large-scale atmospheric circulation patterns such as NAO/AO affect the cyclone activity in the Arctic (Akperov et al., 2019) and impact on local wind characteristics (Laurila et al., 2021). Polar mesocyclones or polar lows are associated with high wind speeds, especially over the Nordic Seas (Rasmussen and Turner, 2003). Local conditions, such as

atmospheric stratification, sea ice concentration, topography or surface roughness (Akperov et al., 2020), affect the spatial and temporal variability of the near-surface wind speed patterns. Therefore, quantifying the variability of the near-surface wind is of particular importance for planning wind farms and safety at sea in general.

Future changes in wind resources were previously examined using data from CMIP5/6 (and respective downscaling from the CORDEX project) for various regions of the Northern Hemisphere under climate change scenarios (Hosking et al., 2018; Li et al., 2020; Carvalho et al., 2021). Most of these studies focus on wind energy resources of specific countries and regions in the midlatitudes (Jung and Schindler, 2022). Due to the low density of the meteorological stations in the coastal zones of the Arctic, as well as in their absence, in particular on the shelf, there are very few or no assessment of regional wind energy resources available. The application of regional climate models (RCM) is one tool to assess the wind energy resources in the Arctic and project the impact of climatic changes on it. Compared to global climate models, RCMs with higher spatial resolution and more detailed surface processes may better capture the near-surface winds, especially in the Arctic (Gutjahr and Heinemann, 2018). Also as shown by Akperov et al. (2018), RCMs can capture cyclone activity and its variability in the Arctic more realistically than their driving Global climate models (GCMs). Therefore, we may expect better surface wind statistics associated with cyclone activity and local conditions by using RCMs. However, it should be noted that there are two well documented main sources of uncertainty associated with RCM assessments: 1) the choice of global climate model used for the boundary conditions; 2) the choice of the RCM itself. Therefore, the use of a multi-model ensemble consisting of different RCMs with different parameterizations and GCM-driven boundary conditions is necessary to assess the robustness of wind resource climate signals. In this study, we analyze an ensemble of Arctic-CORDEX RCMs (<https://climate-cryosphere.org/polar-cordex/>) to assess the sensitivity of wind resources in the Arctic to climate change.

To reduce systematic biases in RCMs, so-called statistical bias correction techniques are applied to RCM output, such as wind speed (Li et al., 2019a). Overall, a bias correction technique for climate projections is based on the comparison of near-surface wind speed between

**Table 1**  
Reanalysis and regional climate models (RCMs), and their corresponding information.

Type	Institution/ Country	Data/ Model name	Original Resolution Vertical levels, horizontal resolution	Boundary conditions	Reference
Reanalyses	ECMWF/UK	ERA5	L137, 0.28 <sup>0</sup> (~ 30 km)		(Hersbach et al., 2020)
Regional climate models (RCMs)	AWI/Germany	HIRHAM5-AWI-MPI	L40, 0.5 <sup>0</sup> (~56 km)	MPI-ESM-LR	(Christensen and Christensen, 2007; Sommerfeld et al., 2015; Klaus et al., 2016)
	DMI/Denmark	HIRHAM5-DMI-EC-EARTH	L31, 0.44 <sup>0</sup> (~48 km)	EC-EARTH2.3	(Christensen and Christensen, 2007; Lucas-Picher et al., 2012)
	SMHI/Sweden	RCA4 -MPI	L40, 0.44 <sup>0</sup> (~48 km)	MPI-ESM-LR	(Berg et al., 2013; Koenigk et al., 2015)
		RCA4-EC-EARTH		EC-EARTH2.3	
		RCA4-CanESM2		CanESM2	
	LU/Sweden	RCA-GUESS-EC-EARTH	L40, 0.44 <sup>0</sup> (~48 km)	NorESM1-M	(Smith et al., 2011; Zhang et al., 2014)
	ULg/Belgium	MAR3.6-NorESM1	L23, 50 km (~0.5 <sup>0</sup> )	EC-EARTH2.3	(Fettweis et al., 2017)
UQAM/Canada	CRCM5-MPI CRCM5-MPIC	L55, 0.44 <sup>0</sup> (~48 km)	MPI-ESM-LR	(Martynov et al., 2013; Šeparović et al., 2013; Takhsa et al., 2017)	
			MPI-ESM-LR (Bias correction) CanESM2		
Global climate models (GCMs)	MPI/Germany	CRCM5- CanESM2 MPI-ESM-LR	L47, 1.8 <sup>0</sup> (~200 km)		(Giorgetta et al., 2013)
	ICHEC/EU	EC-EARTH	L62, 1.1 <sup>0</sup> (~122 km)		(Hazeleger et al., 2012)
	CCCma/Canada	CanESM2	L35, 2.8 <sup>0</sup> (~310 km)		(Arora et al., 2011)
	NCC/Norway	NorESM1-M	L26, 2.5 <sup>0</sup> (~277 km)		(Bentsen et al., 2013)

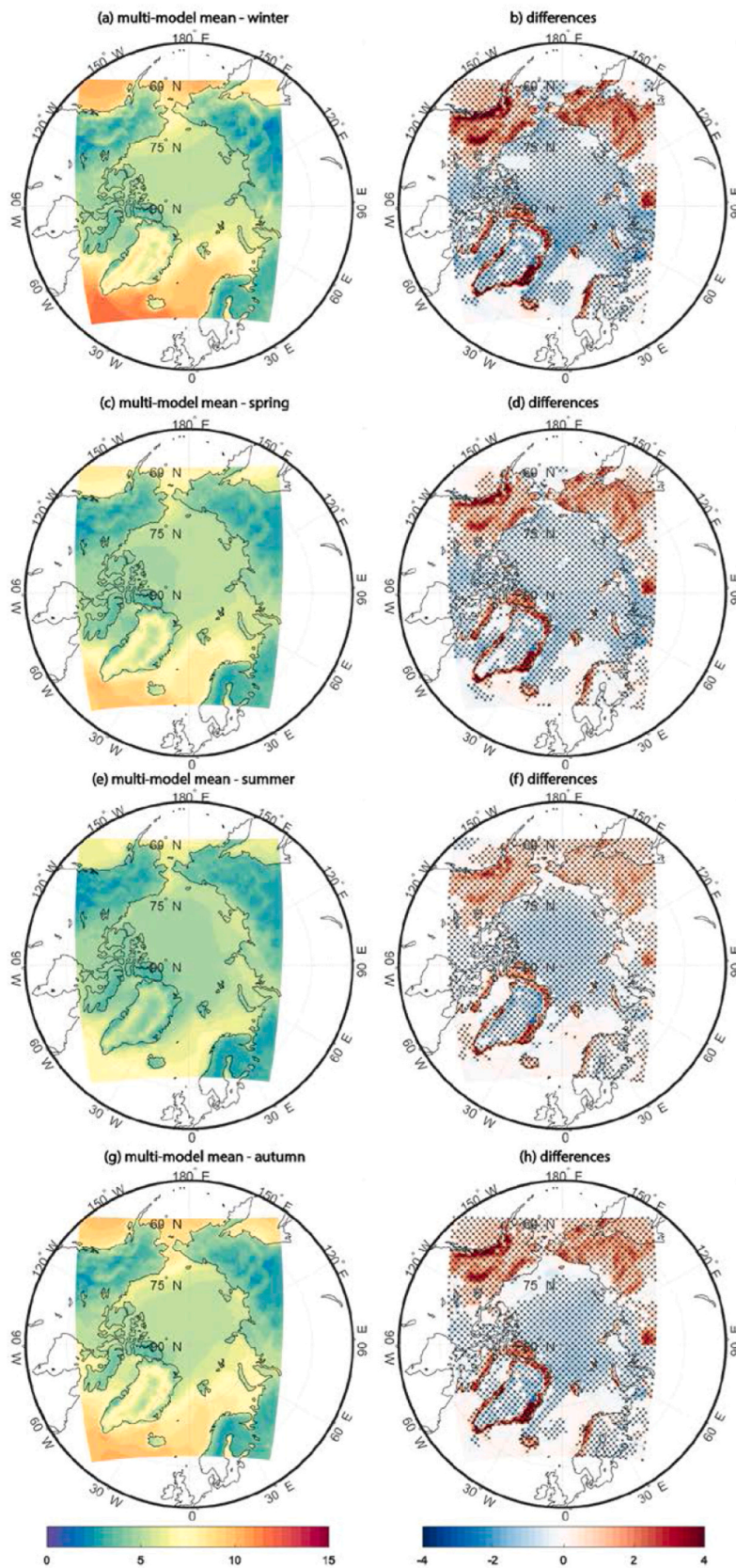


**Fig. 1.** Climatological mean of 10 m wind speed in m/s for multi-model mean for the 1980–2005 for the different seasons and their differences ('multi-model mean' – 'ERA5'). Statistically significant changes ( $p < 0.05$ ) are stippled.

observed and GCM/RCM-simulated variables. A widely used bias correction technique is quantile mapping (QM) (Thiemebl et al., 2011; Gudmundsson et al., 2012; Maraun, 2013), which is based on correcting the shape of the entire variable distribution by establishing statistical relationships between cumulative density functions from the observed and simulated variable (Haas et al., 2014a). We will assess the impact of bias correction on wind speed and wind power density (WPD) changes.

The remainder of the manuscript is organized as follows. In Section 2 we discuss the datasets and methods. In Section 3, we review the model ensemble for consistency with a contemporary reanalysis product, ERA5 (Hersbach et al., 2020). In Section 4, we assess the projected wind speed and WPD changes in the 21st century. In Section 5, we assess uncertainties in WPD projected changes. Finally, we conclude in Section 6.

## 2. Data and methods

### 2.1. Data

We analyze three-hourly mean near-surface (10 m) wind speed data from an ensemble of six atmospheric RCMs (CRCM5, HIRHAM5-AWI, HIRHAM5-DMI, MAR3.6, RCA4, RCA-GUESS) from Arctic-CORDEX, driven by four different GCMs (NorESM1-M, CanESM2, MPI-ESM-LR, EC-EARTH) from CMIP5 and ERA5 reanalysis data (Table 1) for the Arctic region (Fig. 1) for four seasons – winter (DJF), spring (MAM), summer (JJA) and autumn (SON). The GCMs provide lateral and lower boundary (sea surface temperature and sea ice fraction) forcing. The RCMs apply the Arctic CORDEX grid (rotated  $0.44^\circ \times 0.44^\circ$  degrees grid,  $116 \times 133$  grid points).

One of the models (RCA-GUESS) is, in addition, interactively coupled with the vegetation-ecosystem model LPJ-GUESS (Smith et al., 2011; Zhang et al., 2014). RCA-GUESS provides two runs, one with and the other without interactive vegetation-atmosphere coupling, hereinafter denoted as the feedback run (FB) and non-feedback run (NoFB), respectively. FB implements interactive vegetation dynamics in the land surface scheme for the entire simulation period (1961–2100), while NoFB uses fixed land surface properties representing the mean state for 1961–1990, which is similar to how the other RCMs treats the surface interactions. We interpret the difference “FB minus NoFB” as effects by biogeophysical feedbacks (Zhang et al., 2018; Akperov et al., 2021). However, in Sections 3–4 we only use the FB simulation to assess future changes.

Another model (CRCM5-MPIC) represents a run (CRCM5-MPI) with corrected SST. The basic approach of this empirical correction is the assumption that biases in the historical simulation will persist in the future scenario projections. Therefore, the sea-surface conditions simulated by a GCM are empirically corrected by subtracting the biases identified from the historical simulations. More detailed information can be found in Takhsha et al. (2017).

The RCM simulations are driven by the four above-mentioned CMIP5 GCMs for a historical period (from 1950 to 2005) and for a scenario period (from 2006 to 2099) following the high emission scenario (RCP8.5) (Taylor et al., 2012). We have chosen RCP8.5 because multi model data are available for this scenario, but not for others (<https://climate-cryosphere.org/polar-cordex/>). We note that a high end scenario also results in a strong climate response, reducing an additional source of uncertainty related to issues with a signal to noise ratio. We focus our analysis of future wind power density on the 30-year periods 1970–1999 as historical (reference) period and two periods (2020–2049 and 2070–2099) as future periods.

For comparing the RCM results with the reanalysis for the present-day (1980–2005), we use mean three-hourly near-surface wind speed data from the ERA5 reanalysis. ERA5 is the fifth generation of reanalysis from the ECMWF (European Centre for Medium-Range Weather Forecast) (Hersbach et al., 2020). The data cover the Earth on a 31 km grid and resolve the atmosphere using 137 levels from the surface up to a height of 80 km. The ERA5 data have been bilinearly interpolated onto

the Arctic-CORDEX model grid for comparison.

The spatial correlation analysis is based on the Pearson correlation coefficient (R). A nonparametric Mann-Whitney U test (Mann and Whitney, 1947) has been implemented to test for significance of the obtained differences at a 95% confidence level together with an additional false discovery rate correction with  $\alpha = 0.05$  (Benjamini and Hochberg, 1995; Wilks, 2016).

We define a climate change signal to be robust if the following two conditions are fulfilled: more than 75% of model simulations agree on the sign of the change and the signal to noise ratio (SNR), i.e. the ratio of the mean to the standard deviation of the ensemble of climate change signals, is equal to or larger than one. The second criterion is a measure of the strength of the climate change signal (with respect to the inter-model variability in that signal). We use the second criterion in addition to the first, because the first criterion alone may be not sufficient as it may be fulfilled even in the case of a very small, close to zero change (Mba et al., 2018; Nikulin et al., 2018; Akperov et al., 2019).

### 2.2. Wind Power Density

The wind power density (WPD) is an important measure for assessing the potential of wind energy (Nikolaev et al., 2008; Emeis, 2013). It is defined as

$$WPD = \frac{1}{2} \rho u^3, \quad (1)$$

where  $u$  is the wind speed at a given measurement height or adjusted-to-hub height (i.e., the traditional turbine operational height, here 100 m), and  $\rho$  is the air density (take as  $\sim 1.292 \text{ kg/m}^3$ ).

WPD is a measurement of the wind power that is available per unit turbine area ( $\text{W/m}^2$ ). There are several methods commonly used to extrapolate near-surface wind speed measurements to the hub height. One is to use the power law method (Emeis, 2005; Pryor et al., 2005; Hueging et al., 2013; Tobin et al., 2015), which assumes that wind speed at a certain height  $z$  is approximated by

$$u(z) = u(z_r) \left( \frac{z}{z_r} \right)^\alpha, \quad (2)$$

where  $z_r$  is the reference height,  $u(z_r)$  is the wind speed at  $z_r$  and  $\alpha$  is the power law exponent. In our case  $z_r$  is 10 m. Since RCMs do not provide wind speeds at 100 m level as a standard output variable, but only at 10 m height, an extrapolation (such as in Eq. 2) is needed. However,  $\alpha$  has to be known. This is particular critical in the Arctic with its complicated boundary layer structure (Lüpkes et al., 2013). Since ERA5 also provides wind speeds at 100 m, analysis was made to obtain appropriate values of  $\alpha$ . For this purpose, the available ERA5 100 m wind was compared to the extrapolated 100 m using the power-law equation. Finally, we found and applied the following values of  $\alpha$  which minimize the differences between the extrapolated and original 100 m ERA5 winds: 0.18 for land, 0.08 for water; and 0.12 for sea-ice grid points. For the surface condition classification we use the land-sea and sea-ice masks of the respective RCMs. It should be noted that this empirical extrapolation does not account for effects of atmospheric stability or local topography, such as low-level jets, which may play also a role for WPD, since the wind maximum is typically at 100–300 m height (Tuononen et al., 2015; Heinemann et al., 2022).

We correct the biases for near-surface wind speeds in the model simulations using the Weibull distribution-based quantile mapping method (Haas et al., 2014b; Moemken et al., 2018; Li et al., 2019b). The simulated, historical distributions of 3-hourly near-surface wind speed are mapped onto that from ERA5 in order to obtain the transfer function for the bias correction. This transfer function is applied both to the historical and scenario distributions of the near-surface wind speed to obtain the corrected fields. It should be also noted that the quantile mapping method based on Weibull distribution shows the best skills in

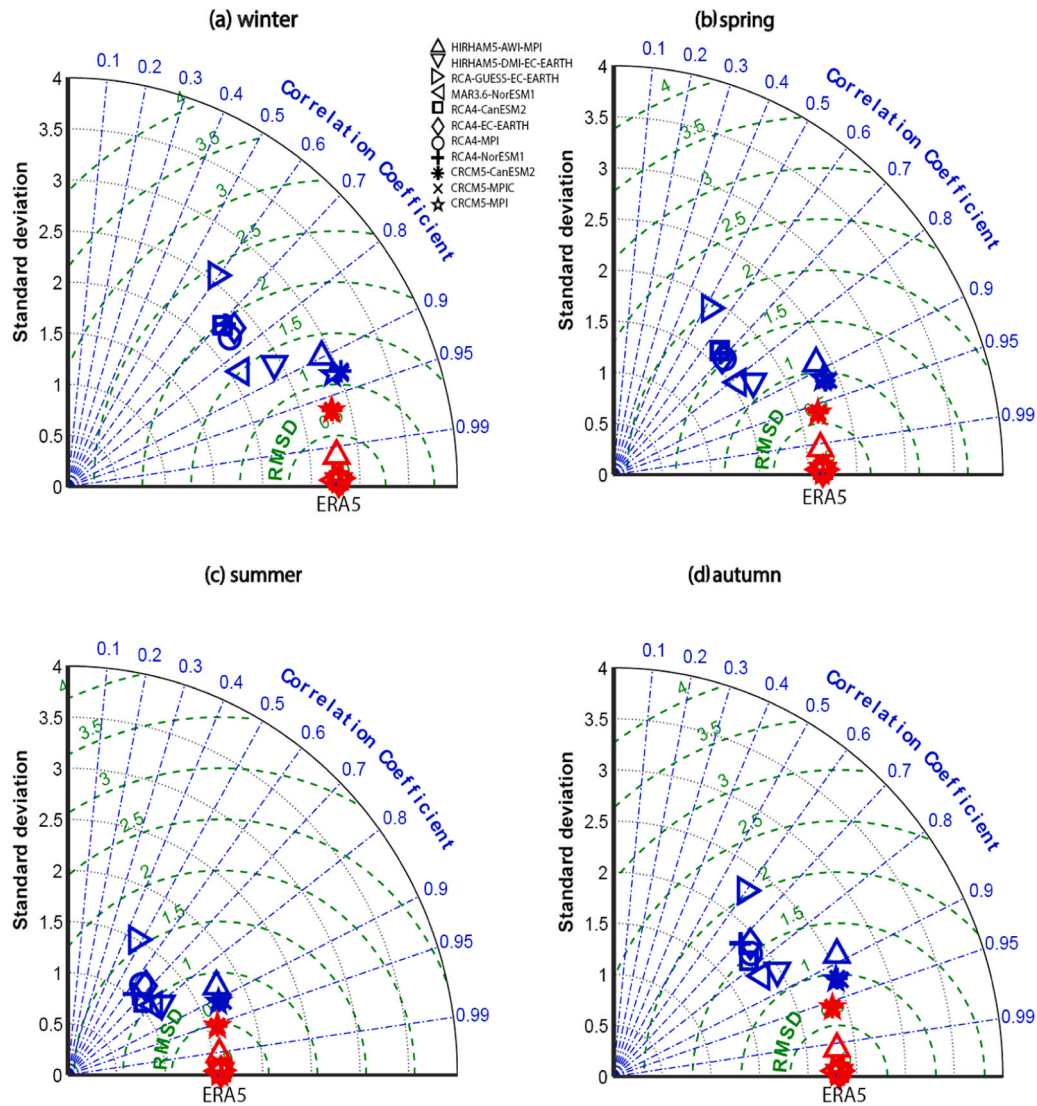


Fig. 2. Taylor diagrams of seasonal mean wind speeds (m/s) from spatially averaged data for ERA5 (reference data) and Arctic-CORDEX simulations for the corrected (red) and not corrected (blue) data temporally averaged during 1980–2005.

bias reduction among other commonly used correction methods (Li et al., 2019b).

Therefore, the bias-corrected near-surface wind speed  $u_{corr}$  can be calculated using the following expression:

$$u_{corr} = c_{era5} \left[ -\ln \left( 1 - \left( 1 - e^{-\left( \frac{u_{model}}{u_{hist}} \right)^{k_{hist}}} \right) \right) \right]^{\frac{1}{k_{era5}}}, \quad (3)$$

where  $u_{model}$  is the near-surface wind speed from RCM,  $c$  and  $k$  are scale and shape parameters of the cumulative Weibull distribution for near-surface wind speeds from ERA5 reanalysis and from RCM for the historical period (hist). Historical shape and scale parameters are used for the correction of both historical runs and future projections for the computation of WPDs.

Finally, we analyze future changes in the frequency of wind speeds at 100 m not useable for wind energy production (both with and without bias correction). These are very relevant for the wind energy exploitation industry since the current wind turbines cannot produce energy from wind flows with speeds below 4 m/s (called the cut-in speed) or above 25 m/s (cut-off speed) (Carvalho et al., 2021). To assess these changes, the difference between the historical and future periods in the number of days per year with wind speeds at 100 m below/above these

thresholds were analyzed.

Throughout the text we focus on not corrected WPD and wind speed, except in Section 5.1 where we discuss the effect of bias correction on WPD and wind speed changes.

### 3. Comparison of near-surface wind speeds from historical simulations and ERA5 reanalysis

The surface winds from ERA5 exhibit the best agreement amongst the modern reanalyses with in situ observations in midlatitudes and Arctic (Graham et al., 2019; Ramon et al., 2019; Minola et al., 2020) and are widely used for assessments of wind energy resources for the different areas (Lambin et al., 2023; Olauson, 2018; Soares et al., 2020). Furthermore, as previously noted, there is a lack of quality wind observations over most of the Arctic-CORDEX domain. Therefore, we use near-surface wind speeds from ERA5 as the reference data in our analysis. However, we are aware that all reanalysis data (incl. ERA5) have limitations in representing local conditions (Dörenkämper et al., 2020; Gruber et al., 2022).

Here we compare the near-surface wind speed climatology from the multi-ensemble mean of historical runs and ERA5 reanalysis for the period 1980–2005. Fig. 1 shows the near-surface wind speed

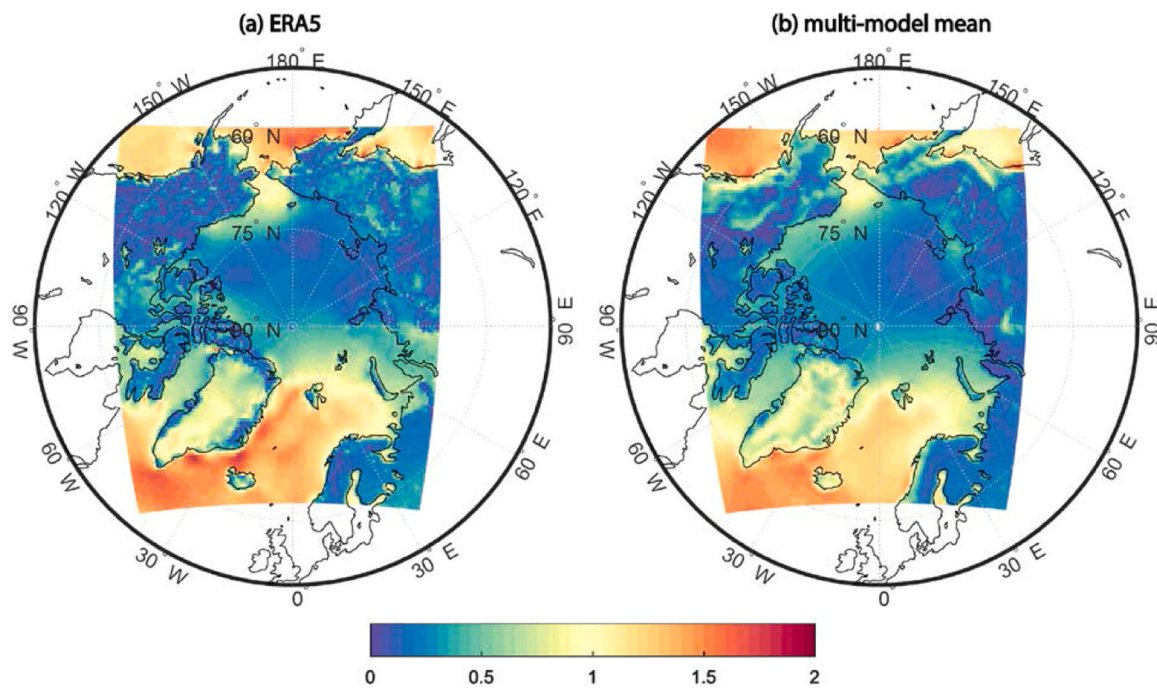


**Fig. 3.** Intraannual variability of near-surface wind speed (m/s) of ERA5 (a) and multi-model mean (b).

climatology from the ERA5 reanalysis and the multi-model mean as well as their differences for the four seasons (DJF, MAM, JJA, and SOM) in the Arctic. For all four seasons, higher values of wind speed in the multi-model mean are found over the continents and lower values over the Arctic Ocean compared to ERA5. Despite quantitative differences, the Arctic-CORDEX models reproduce the spatial distribution of near-surface wind speed over the Arctic with a maximum over the Nordic Seas (the region of highest cyclone activity) and minimum over the continents for all four seasons. To examine the performance of Arctic-CORDEX model runs in representing mean near-surface wind speeds with respect to ERA5, we apply Taylor diagrams (Fig. 2). The spatial correlation coefficients ( $R$ ) between the individual models and ERA5 reanalysis near-surface wind speed range from 0.59 (RCA-GUESS) to 0.93 (CRCM5-MPIC) for winter, from 0.52 (RCA-GUESS) to 0.92 (CRCM5-MPIC) for spring, from 0.47 (RCA-GUESS) to 0.91 (CRCM5-MPIC) for summer and from 0.6 (RCA-GUESS) to 0.93 (CRCM5-MPIC) for autumn. The spatial standard deviations (SDs) for RCMs lie in the range from 2.1 to 3.0 in winter, from 1.6 to 2.4 in spring, from 1.1 to 1.7 in summer and from 1.8 to 2.5 in autumn. Respective root-mean-square deviations (RMSDs) vary from 1.1 to 2.5 for winter, from 0.9 to 1.9 for spring, from 0.7 to 1.6 for summer and from 0.9 to 2.1 for autumn. The possible reason for the high correlation of CRCM-MPIC with ERA5 is the correction of the SST (boundary forcing from GCM MPI-ESM-LR) in CRCM5-MPIC, which improves the atmospheric circulation (Akperov et al., 2019). This leads to a better representation of the near-surface wind speed in the Arctic. In the case of RCA-GUESS (low correlation with ERA5), the differences are also related to the boundary forcing (EC-EARTH). EC-Earth has a cold bias in summer and a warm bias in winter and spring (Fig. 2 in Zhang et al., 2014). Fig. 10b in (Koenigk et al., 2013) also shows the mean sea level pressure (MSLP) biases between EC-EARTH and reanalysis over the Arctic (positive biases in areas from Alaska across the Bering Strait towards Siberia and negative biases over the European Arctic). Therefore, it may affect the circulation, including the near-surface wind speed, and lead to a low correlation with ERA5.

Fig. 3 shows intra-annual variability (standard deviation of seasonal means of near-surface wind speed) of near-surface wind speed from ERA5 and multi-model mean. Overall, both ERA5 and the multi-model

mean show similarity in terms of intra-annual variability with strong regionally different patterns for near-surface wind speed, in particular strong seasonality over ice-free ocean and weak over land and ice-covered Arctic (Fig. S1).

Overall, the historical runs show substantial differences compared to the ERA5 reanalysis. These differences are most pronounced over areas of complex topography (East Greenland and Norwegian coasts, south Alaska, over the ocean along the coast of East Greenland) and may be associated with improvement of local topography and wind systems, such as katabatic winds or wind gusts in RCMs. But they can be also associated with biases from the driving GCMs, especially over the sea ice areas (which deviates substantially from the observed most prominently in the vicinity of the observed sea ice edge) and from the RCM physics. These biases influence the climate change signal, in particular wind speed thresholds, which are relevant for wind energy production. To estimate the impact of bias correction on near-surface wind and WPD changes, we performed the analysis both with and without bias correction technique. As shown in Fig. 2, corrected 10 m wind speeds are very close to ERA5 for all seasons compared to the uncorrected data. However, further analysis in Section 4 focuses on not corrected wind speed and WPD changes, while in Section 5, we assess the role of bias-correction on WPD and wind changes.

#### 4. Future changes of wind speeds and wind power density

The future responses of WPD are analyzed for the RCP8.5 scenario for the two periods (2020–2049 and 2070–2099). We investigate future changes of seasonal WPD, which could be important for the planning of future wind farms.

The projected changes of the seasonal WPD from the multi-model mean are presented in Figs. 4 and 5. In winter and spring, the areas of the strong increase of WPD are located over the eastern Barents and Kara Seas which are related to the projected strong sea ice retreat in these marginal seas. Additionally, WPD increases in the Greenland, Chukchi and Bering Seas. However, WPD decreases over the Norwegian Sea and western Barents Sea. In summer and autumn, a strong increase of WPD is calculated over the northern Barents, Kara, and Greenland Seas and along Arctic near-shore zones as well as Arctic Ocean in 2070–2099.

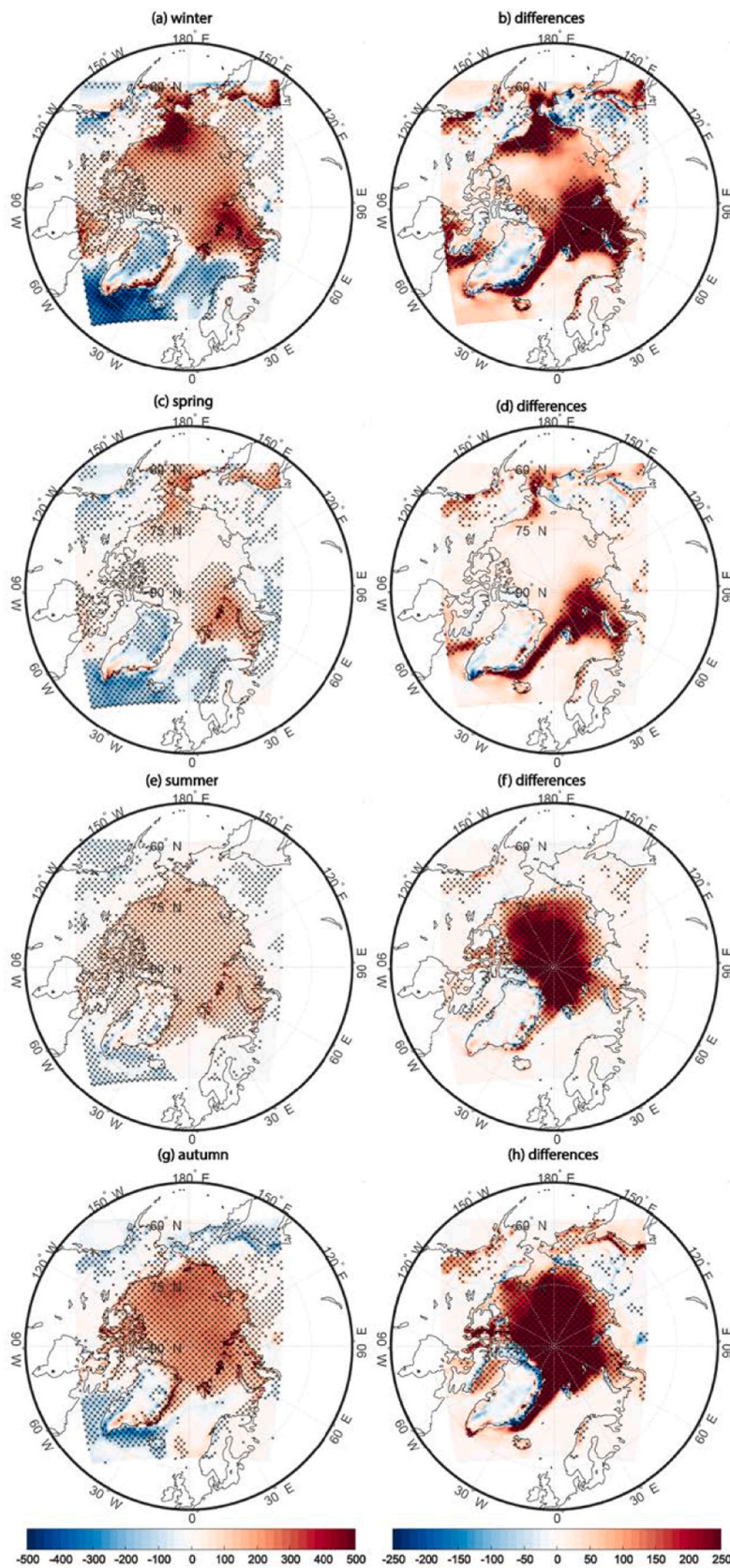


**Fig. 4.** Changes of not corrected seasonal mean WPD ( $W/m^2$ ) for multi-model means in 2020–2049 with respect to 1970–1999 (a,c,e,g). Panels (b,d,f,h) show differences between bias-corrected and not corrected fields for the corresponding figures and seasons (a,c,e,g). Statistically significant changes ( $p < 0.05$ ) are stippled.

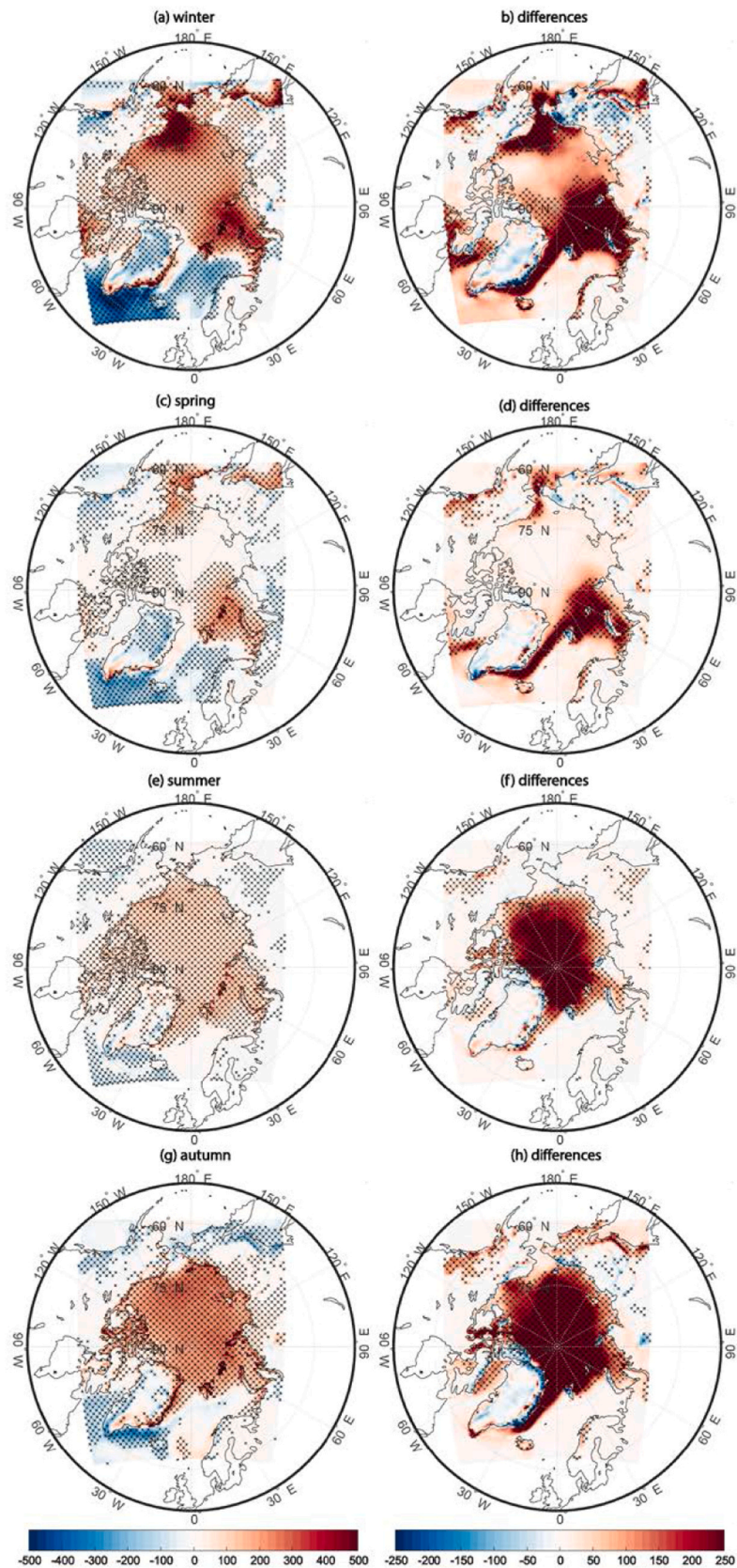


**Fig. 5.** Changes of not corrected seasonal mean WPD ( $W/m^2$ ) for the multi-model means (2070–2099) with respect to historical period (1970–1999) (a,c,e,g). Panels (b,d,f,h) show differences between bias-corrected and not corrected fields for the corresponding figures and seasons (a,c,e,g). Statistically significant changes ( $p < 0.05$ ) are stippled.

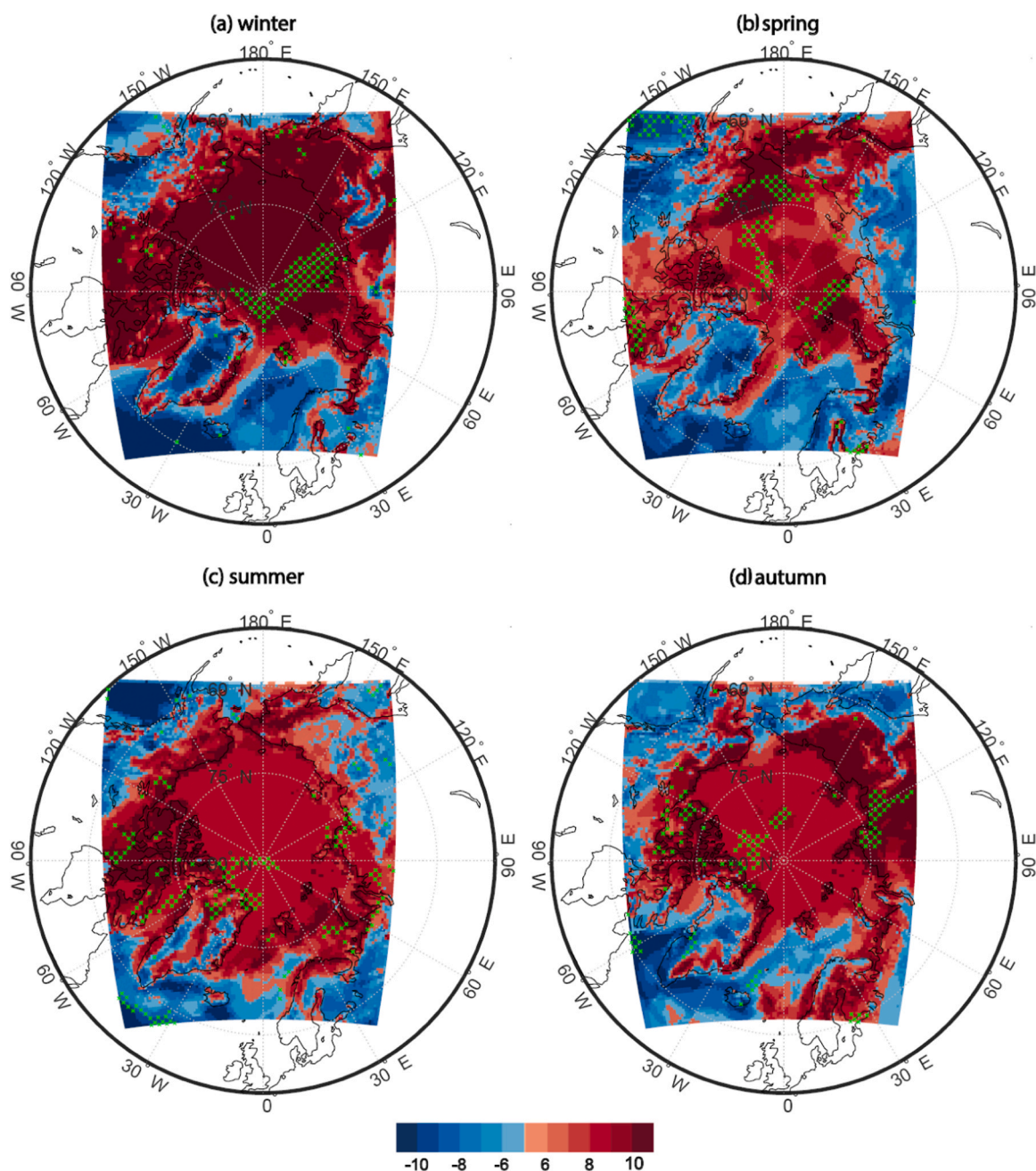


**Fig. 6.** The number of not corrected models, which show the same sign changes of WPD for 2070–2099 relative to 1970–1999. Red colors indicate positive changes and blue stand for negative ones; if models simulate changes of different signs, the maximal number of models showing same sign changes is shown. Areas where at least 8 of 11 models agree on the sign of the change and signal to noise ratio (SNR) is larger than 1 are marked by green dots.

This is associated with projected strong sea-ice retreat there (Fig. 11). Reduction of WPD is noted over the southern Barents Sea. It is noted that models simulate also a strong increase of WPD over the Arctic Ocean in winter in 2070–2099, irrespectively of small sea ice reduction and the related minimal warming in this area. According to Fig. 6, for the end of the century, all models agree on the positive sign of WPD changes over the Arctic Ocean, including parts of Barents Sea, Greenland and Chukchi Seas, and along Arctic near-shore zones in all seasons and the negative sign in the ice-free Barents and Norwegian Seas in winter, spring and autumn. These findings are consistent with the research conducted by Vavrus and Alkama (2021), who utilized near-surface wind speed data from an ensemble of climate models sourced from CMIP5 under RCP8.5 (their Figs. 4 and 5).

Further, we analyze changes in the variability of WPD, ranging from

intra-annual to inter-daily timescales. These timescales are of high importance for the production and operation of the energy system and the integration of wind energy into the energy system (Moemken et al., 2018). The inter-daily timescales are relevant for the power system management and energy trading, and intra-annual to inter-annual timescales are important for resource assessments and the planning of backup and storage facilities.

The seasonal changes of WPD (as shown in Figs. 4 and 5) lead to an ensemble mean amplification of the intra-annual variability of WPD (standard deviation of seasonal means of near-surface wind speed) over the Arctic Ocean and the Arctic near-shore regions (Fig. 7). All seasons except summer contribute markedly to the changes shown in Fig. 7. While in 2040–2060 the maximum increase is over the northern Barents, Kara, and Greenland Seas, in 2070–2099 the increase reaches up to

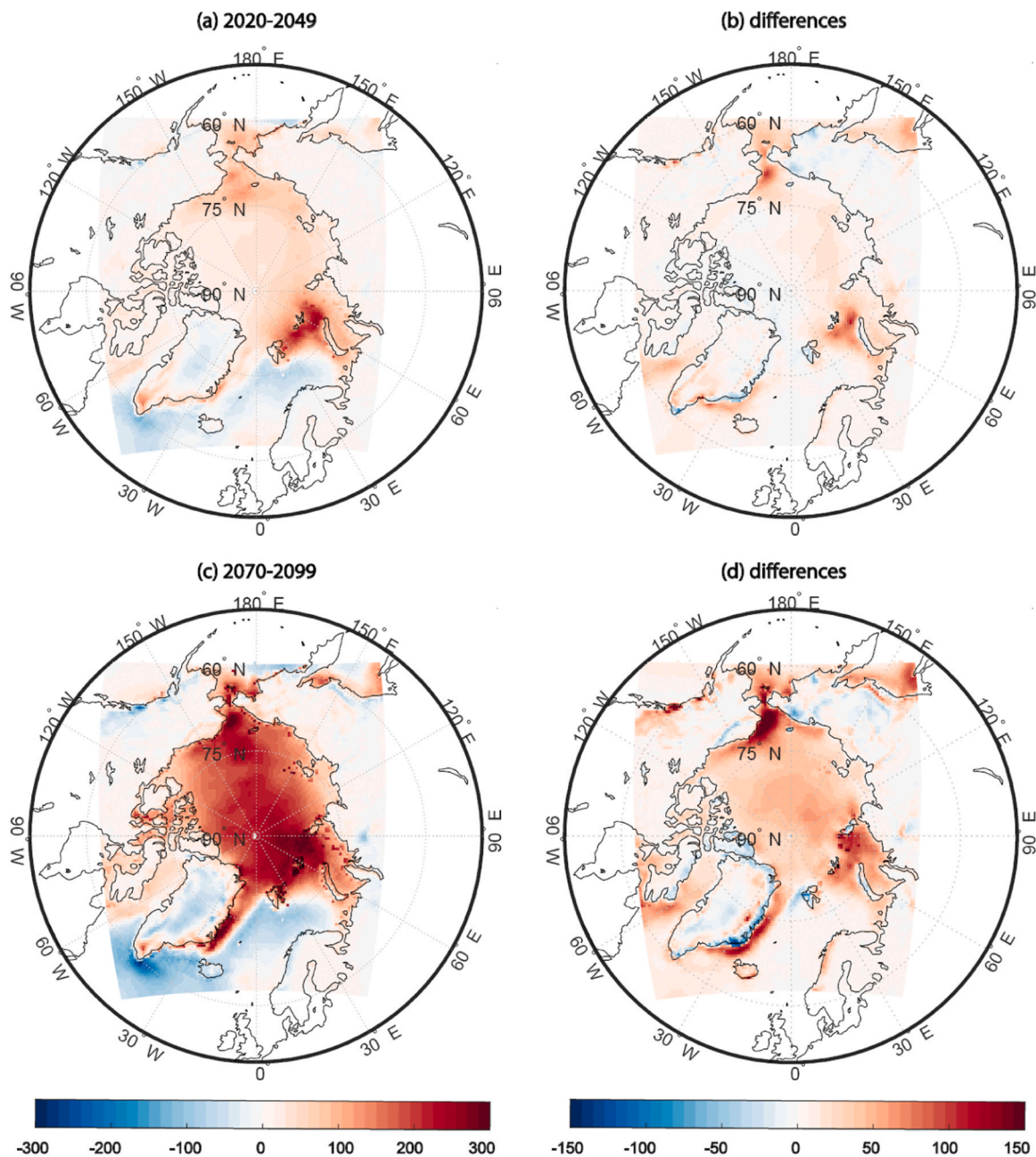


Fig. 7. Changes of intra-annual variability of not corrected WPD ( $\text{W}/\text{m}^2$ ) for the multi-model mean of RCP8.5 for the two periods (2020–2049 and 2070–2099) with respect to historical period (1970–1999) (a,c). Panels (b,d) show differences between bias-corrected and not corrected fields for the corresponding figures (a,c).

$300 \text{ W}/\text{m}^2$  over the northern Barents-Kara and Chukchi Seas.

Changes in the inter-annual variability (standard deviation of annual WPD values in a given period) are presented in Fig. 8. As for intra-annual variability, a remarkable increase of WPD is seen over the northern Barents-Kara, Greenland and Chukchi Seas by the end of 21st century. In contrast, a weak decrease is seen over the southern Barents Sea. The maxima of both intra- and inter-annual variability of WPD are located near the sea ice boundary. Thus, we conclude that they are related to the same driver – the receding sea ice. However, because other drivers for their changes are possible as well, we do not conclude on close relations between the intra- and inter-annual variability.

Fig. 9 shows the future projections for the inter-daily variability of WPD (standard deviation of averaged daily WPD values) for the model ensemble mean for the RCP8.5 scenario. Inter-daily variability of WPD also increases with remarkable changes over the northern Barents and Kara Seas, and Arctic near-shore regions by the end of the 21st century.

However, there is a slight decrease over the Nordic Seas in both periods.

Fig. 10 shows the projected changes in the number of occurrences of 3-hourly periods per year for the 100 m wind below cut-in (4 m/s) or above cut-off (25 m/s) speeds under the RCP8.5 scenarios. This range of wind speed represents the non-usable wind for the energy production for the current generation of wind turbines. According to Fig. 10, the future climate projections show increased occurrences of non-usable wind speeds over Scandinavia and selected land areas in Alaska, northern Russia and Canada. A decrease of non-usable wind speeds is calculated over the large part of Eastern Siberia and in northern Alaska. These changes are mainly due to wind speeds below 4 m/s (not shown). In general, the changes amplify by the end of 21st century. On the other hand, there are no projected changes of non-usable wind speeds over the Arctic Ocean including Arctic near-shore zones where WPD increases in all seasons by the end of 21st century (Figs. 4 and 5).

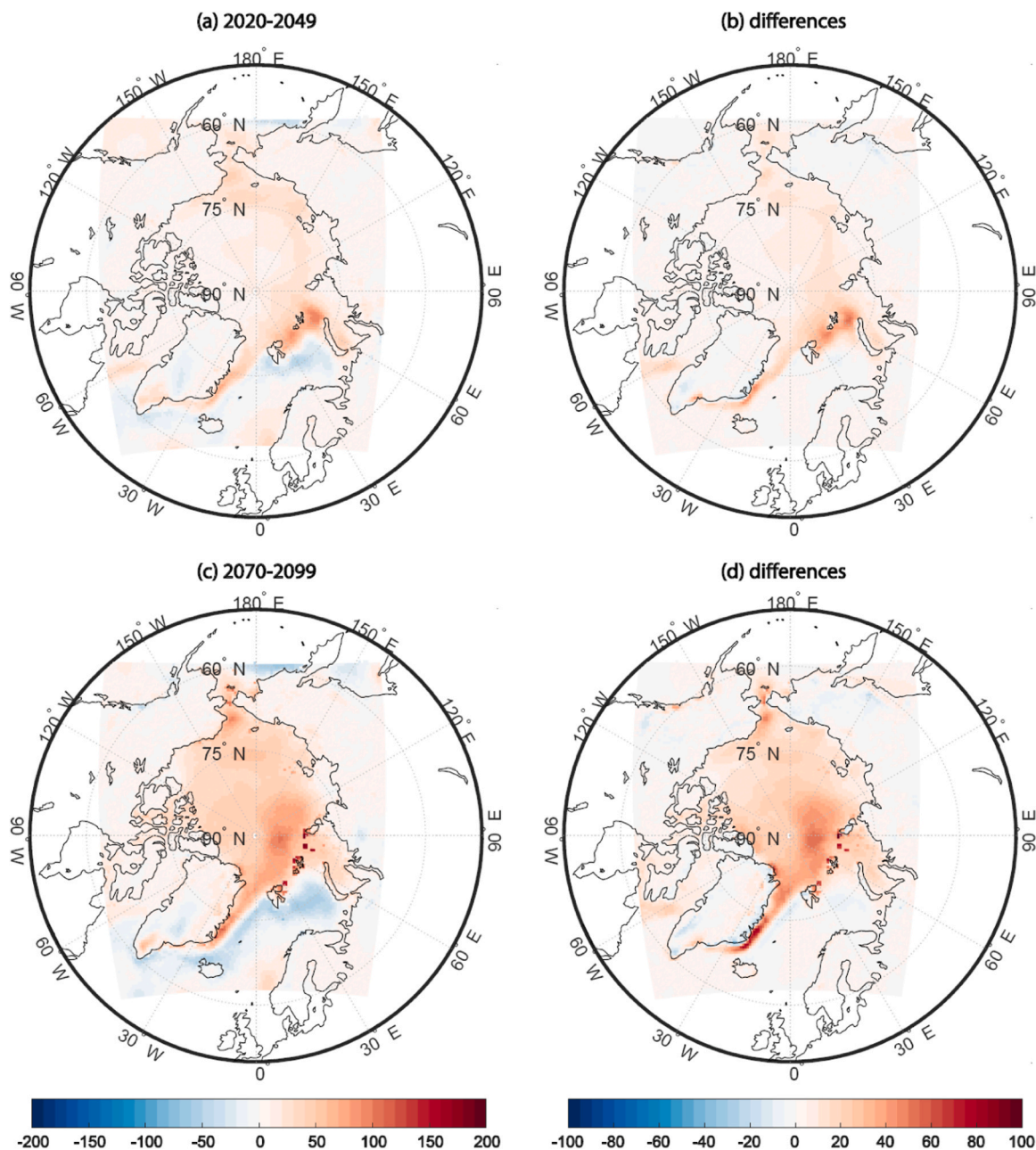


**Fig. 8.** Changes of inter-annual variability of not corrected WPD ( $\text{W}/\text{m}^2$ ) for the multi-model mean for two periods (2020–2049 and 2070–2099) with respect to historical period (1970–1999) (a,c). Panels (b,d) show differences between bias-corrected and not corrected fields for the corresponding figures (a,c).

## 5. Uncertainties in WPD future changes

### 5.1. Bias correction

The sensitivity of WPD projections to the bias correction method is analyzed by calculating the difference between corrected and not corrected WPD changes (Costoya et al., 2020). Significant differences between corrected and not corrected WPD are seen in the ocean regions of strong WPD changes (Figs. 4 and 5). WPD based on bias-corrected data are generally increased compared to using non-corrected data. The increase in WPD by using bias-corrected wind data can reach 50%. In winter and spring, the areas of strong differences between corrected and not corrected WPD are located in particular over the Barents-Kara, Greenland and Chukchi Seas. Also in summer and autumn, significant WPD differences occur over the Arctic Ocean including Arctic near-shore areas. These differences partly reflect the greater loss of sea ice in these

sub-regions (see also Section 5.2). The WPD differences over land are generally small, and show up especially over areas of complex terrain (e. g., Greenland and coastal regions). The inspection of the intra-annual, inter-annual and inter-daily WPD differences (Figs. 7, 8 and 9) show that the bias-corrected data lead to an increase of the WPD variability. Overall, both bias-corrected and not corrected WPD changes show the same sign of future change, but differ in the magnitude of these changes.

Fig. 10 shows that remarkable changes are noticed over the areas of complex terrain. Corrected data shows a reduction of the frequency of non-usable wind speeds over the Alaska, Far East and other land areas over Russia. Increasing frequency of non-usable wind speeds is seen over Scandinavia and over land areas in eastern Siberia.

### 5.2. Impact of surface conditions

One of the key factors influencing the near-surface wind speed in the

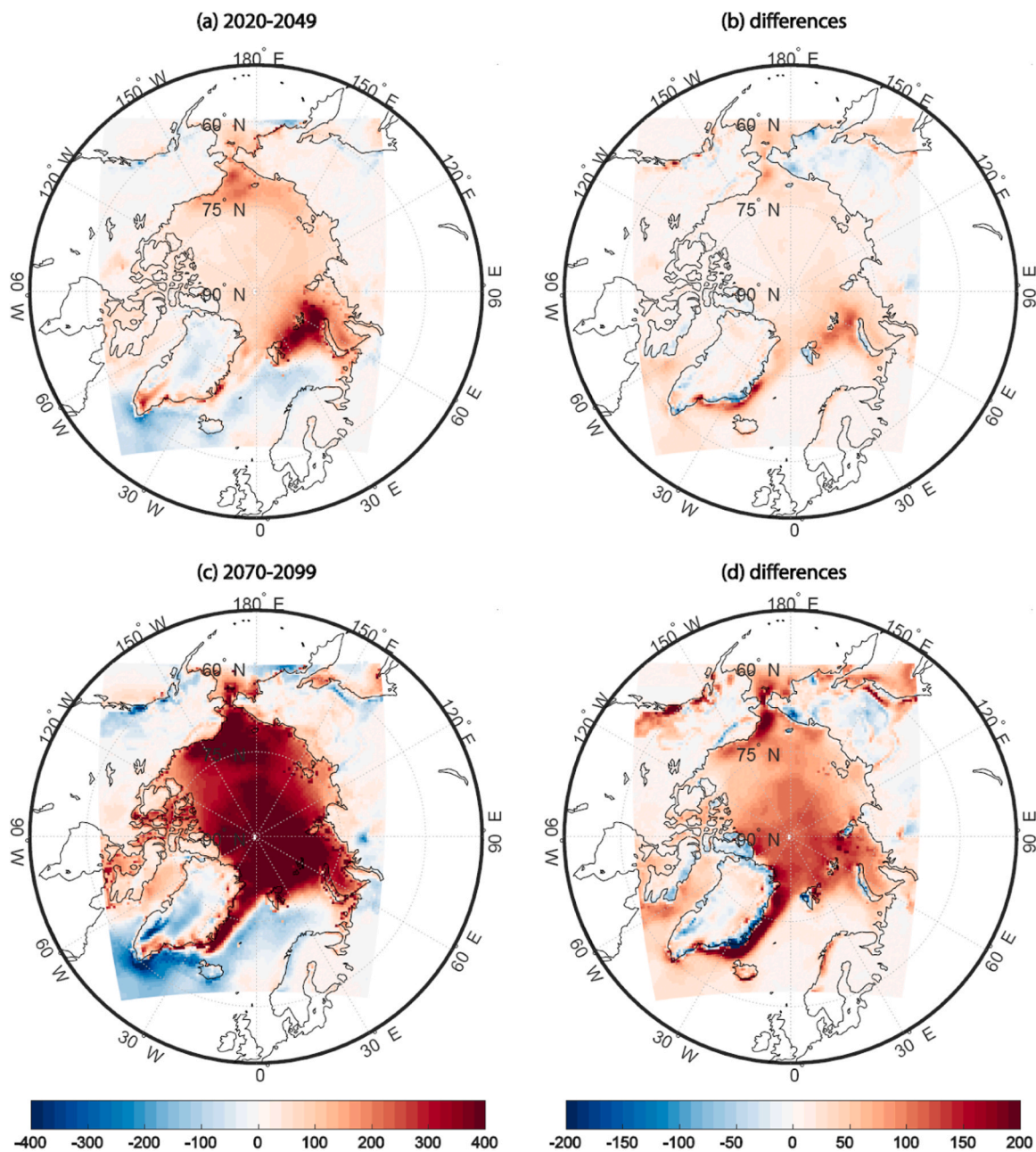
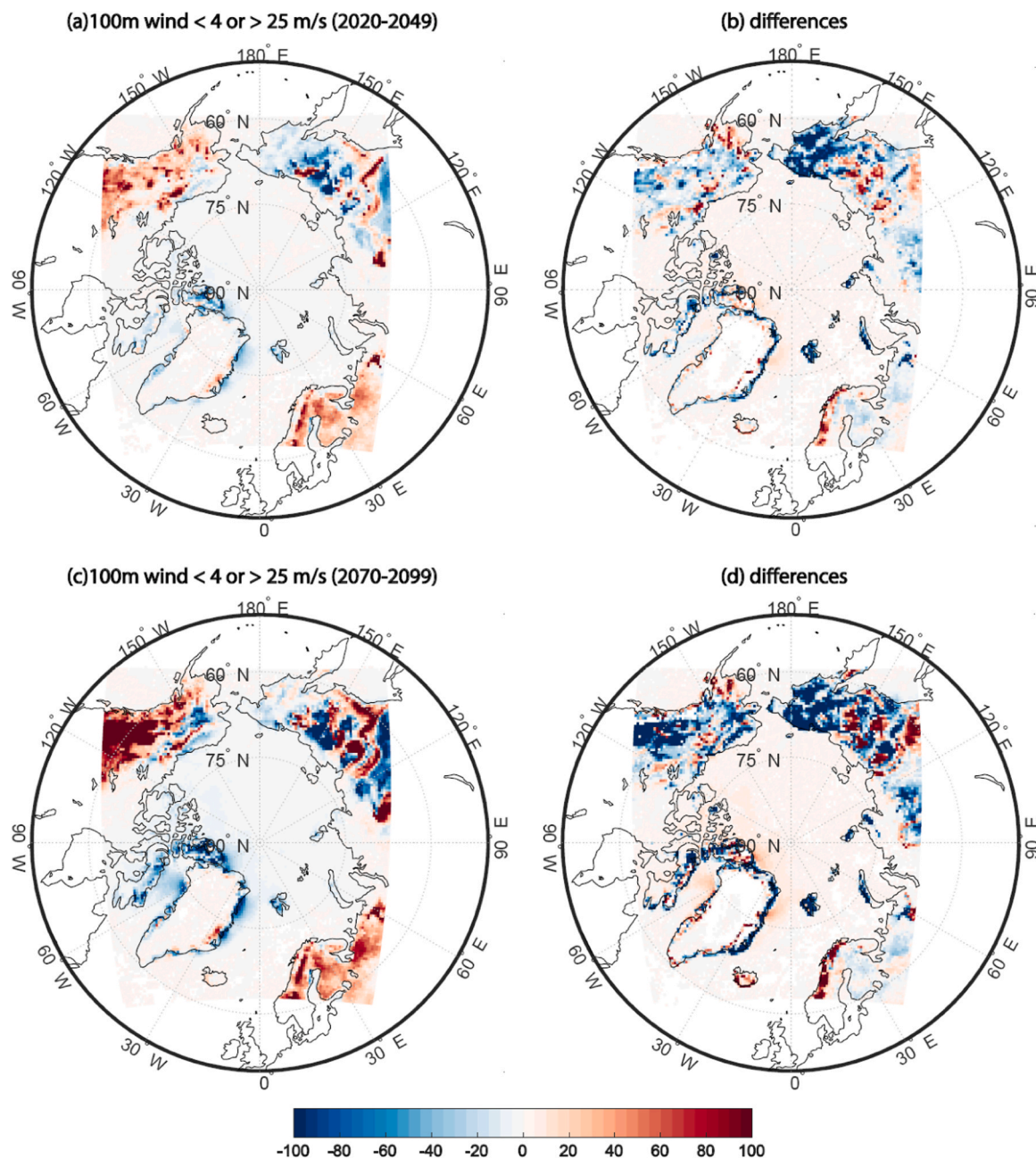


Fig. 9. Changes of inter-daily variability of not corrected WPD ( $W/m^2$ ) for the multi-model mean for two periods (2020–2049 and 2070–2099) with respect to multi-model mean of historical (1970–1999) (a,c). Panels (b,d) show differences between bias-corrected and not corrected fields for the corresponding figures (a,c).

Arctic in future is the sea ice reduction, which affects the aerodynamic surface roughness and stratification in the Arctic atmosphere. As was reported earlier (Mioduszewski et al., 2018; Jakobson et al., 2019; Vavrus and Alkama, 2021), reduction in ocean surface roughness caused by a transition from ice-covered to open water ocean and associated reduced atmospheric stability due the enhanced surface warming led to a strengthening of near-surface wind speeds in the Arctic. This, in turn, further affects the WPD changes. We confirm that the drastic sea ice loss in the Arctic including Arctic near-shore zones in all seasons by the end of 21st century (Fig. 11) is associated with a strong increase of WPD magnitude and variability over these areas (Figs. 5, 7–9).

Regarding the land areas, Arctic warming changes, such as shrubification and the latitudinal and altitudinal shifts of tree-line, may change the fractional coverage of different vegetation types. This leads to a positive surface temperature feedback associated with lowered surface albedo and to a negative feedback associated with higher

evapotranspiration (Eliseev and Mokhov, 2011; Pearson et al., 2013; Zhang et al., 2014, 2018). And this, in turn, leads to changes in static stability, atmospheric circulation through the changes in thermal meridional gradient and surface roughness through vegetation extent (Zhang et al., 2014, 2018; Akperov et al., 2021), and, therefore, may impact on near-surface wind speed and WPD changes over the land. Using RCA-GUESS simulations with (FB) and without (NoFB) interactive vegetation–atmosphere coupling, we assessed an impact of roughness changes (from vegetation expansion) on WPD. The strongest changes in near-surface air temperature are observed in spring and summer (Zhang et al., 2014), therefore, both seasons have been chosen for the further analysis. Fig. 12 shows spatial distribution of various variables between FB and NoFB simulations. The warming in spring and cooling in summer is in accordance with the above described feedbacks. Further, the vegetation changes (Arctic greening) over the land significantly impact on the near-surface wind speed as well as WPD in both seasons. The WPD



**Fig. 10.** Changes in the number of three-hourly dates per year with (a,b) not corrected 100 m wind speed < 4 or > 25 m/s from the multi-model mean of RCP8.5 for the two periods (2020–2049 and 2070–2099) with respect to multi-model mean of historical (1970–1999). Panels (b,d) show differences between bias-corrected and not corrected fields for the corresponding figures (a,c).

is significantly reduced over the lands due to enhanced vegetation (increasing surface roughness). The reduction in WPD over the land by using changing vegetation can reach 100% (500 W/m<sup>2</sup> in spring and 250 W/m<sup>2</sup> in summer). These changes are comparable to those over the Arctic Ocean and exceed biases between not corrected and corrected WPD (Fig. 5).

While WPD is reducing over the land in both seasons, static stability (which is expressed by the vertical difference in the temperature between 850 hPa and near-surface temperature) has a different behavior over the continents in spring and summer. In spring, static stability decreases, whereas it increases in summer. As was shown in (Akperov et al., 2021), changing vegetation leads to a mean sea level pressure reduction (increase in cyclonicity which can lead to increased near-surface wind speed) over the continents in both seasons. Both factors should increase near-surface wind speed and WPD. However,

near-surface wind speed decreases over the continents in both seasons (Fig. 12). Therefore, surface roughness through vegetation expansion on wind speed and WPD variability over the continents may be seen as a key factor in controlling the wind speed.

We may conclude on significant uncertainties related to the estimation of future changes in WPD. Both the sea-ice retreat and the vegetation expansion influence wind speed. At the same time using bias correction significantly changes the wind energy potentials in the Arctic in the future.

## 6. Summary and conclusion

Our work presents an assessment of wind energy resources and associated spatiotemporal patterns over the Arctic using regional climate model simulations from the Arctic-CORDEX initiative within an

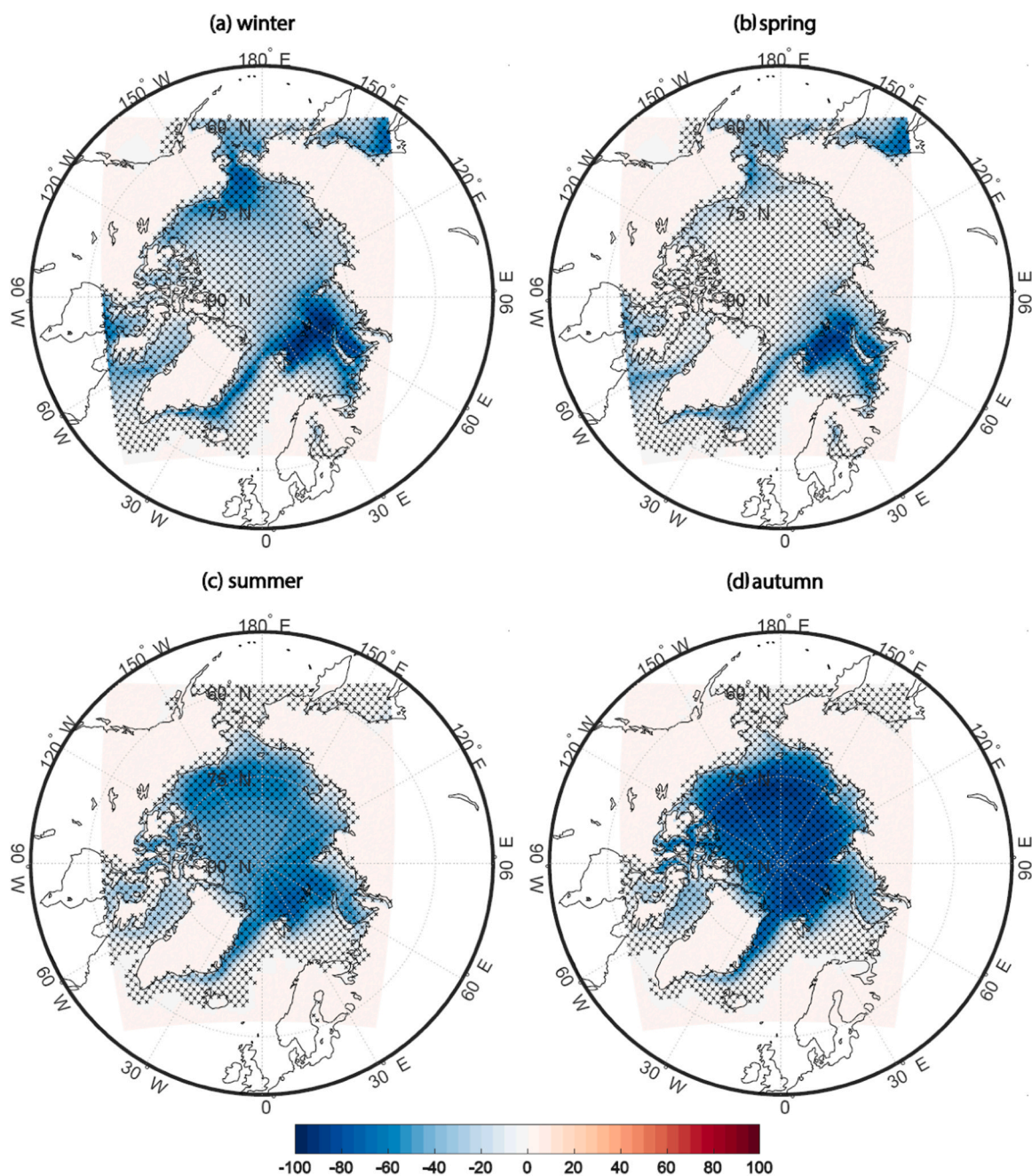


**Fig. 11.** Changes in sea-ice concentration (%) for the multi-model mean of driving GCM's for RCP8.5 for the 2070–2099 with respect to multi-model mean of historical period (1970–1999) for the different seasons. Statistically significant changes ( $p < 0.05$ ) are stippled.

RCP8.5 scenario for the 21st century. The multi-model mean projections reveal an increase of seasonal WPD over the Arctic in the future decades. In winter and spring, the areas of the strong increase of WPD are located over the eastern Barents, Kara, Greenland, Bering and Chukchi Seas. WPD decreases over the Norwegian Sea and western Barents Sea. In summer and autumn, WPD increases over the northern Barents, Kara, and Greenland Seas and along Arctic near-shore zones as well as Arctic Ocean in 2070–2099. The signals become stronger by the end of 21st century. However, increasing WPD variability in future decades will lead to a higher irregularity of wind energy production.

The RCM ensemble exhibits a more frequent occurrence of 100 m non-usable wind speeds over Scandinavia, northern Russia, Canada and selected land areas in Alaska in the future climate. In contrast, non-usable wind speeds decrease over the large part of Eastern Siberia and in northern Alaska. All changes of the non-usable wind speeds occur

over the land areas and away from the coastal zone.

We quantify the sensitivity of WPD projections to the bias correction by calculating the difference between bias-corrected and not corrected WPD changes. The increase in WPD by using bias-corrected wind data can reach 50%. The areas of strong differences between bias-corrected and not corrected WPD are located over the WPD seasonal increase and decrease. Overall, because both bias-corrected and not corrected WPD changes show the same sign of future change, the sign of the response in our paper is credible. However, the respective magnitude remains uncertain. We note, however, that bias correction (as well as any statistical post-processing procedure) is unlikely able to improve possible model shortcomings in projecting a non-linear response of wind to climate forcing. On the other hand, some credibility for our results is provided by the absence of such nonlinear response in large-scale forcing data.

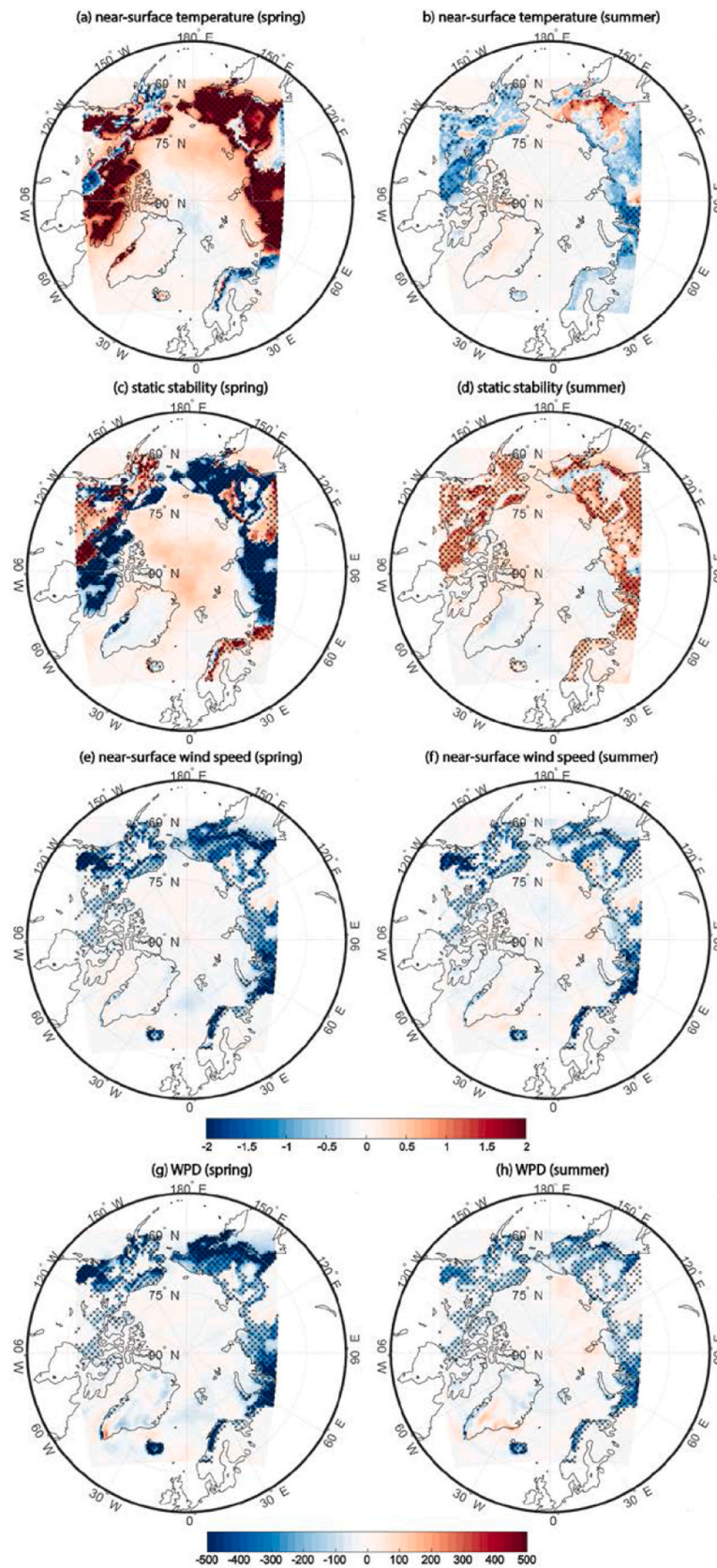


**Fig. 12.** The effects of biogeophysical feedbacks on near-surface temperature [K] (a,b), static stability [K] (c,d), near-surface wind speed [m/s] (e,f) and WPD [W/m<sup>2</sup>] (g,h) for the different seasons averaged from 2070 to 2099 with respect to historical period (1970–1999). Statistically significant changes ( $p < 0.05$ ) are stippled.

The increase in variability of the bias-corrected WPD/wind speed relative to the uncorrected data in the future climate, especially over the sea ice reduction areas, can be explained by several factors. Firstly, the correction depends on the quality of the reference data that is used for the correction. If coarser data (such as ERA5) is used, then errors could be introduced where the higher resolution of the RCMs would be beneficial, e.g. over the steep topography of Greenland. Secondly, the transfer functions are commonly assumed to be constant over time, so that they hold also for future climates. Such assumption is unavoidable lacking future ‘observations’ and used in any prognostic statistical model. If that is true is very uncertain, in particular in areas where sea ice is retreating, which would affect the transfer functions. Concluding, bias correction is just a statistical short-cut with large uncertainties. Therefore, we focused on discussing bias-corrected versus uncorrected results.

The role of sea-ice retreat and vegetation expansion on near-surface wind speed and WPD variability has been also assessed. Reduction in ocean surface roughness caused by a transition from ice-covered to open water and reduced atmospheric stability and greater vertical momentum mixing due the enhanced surface warming lead to strengthening near-surface wind speeds over the Arctic with the most pronounced effect in winter-autumn. Similarly, the near-surface wind speed as well as WPD significantly decreases over the continents due to increasing vegetation extent (surface roughness) in biogeophysical feedback simulations in spring-summer.

Estimations of the future WPD changes suffer from different kinds of uncertainty. These are related to changes of the air density, which is expected to decrease due to near-surface temperature increase. Especially, it is expected to have an effect over the Barents Sea (Koenigk et al., 2013). However, a contribution of air density changes to WPD will be much smaller compared to changes in near-surface wind speeds. Other uncertainties are related to the height of future wind turbines, which is expected to be higher than the current generation of turbines (McKenna et al., 2016), and - although not addressed in this work - to the considered emission scenario.

We analyzed the RCP8.5 scenario, which is high emission scenario. The number of the available CORDEX simulations is the largest for this particular RCP scenario. This allowed us to highlight the strongest possible changes by the end of the 21st century. Again, we note that the results of low (RCP2.6) and high emission scenarios are very similar for the near future of two-three decades - but differ substantially for the end of the 21st century.

We note that the CMIP5/6 ensemble of GCMs appear to be biased when it comes to the retreat of Arctic sea ice (Massonnet et al., 2012; Collins et al., 2013; Koenigk et al., 2015; Eliseev and Semenov, 2016; Docquier and Koenigk, 2021) In particular, it has been demonstrated that future scenarios of sea ice retreat building on CMIP5 only match current rates of Arctic change in GCMs following a scenario with greater warming than RCP4.5, with few exceptions (Jansen et al., 2020). The current suite of driving GCMs has not been chosen with this in mind, which may imply that even end of century projection of WPD may be better captured using RCP8.5 than lower emission scenarios even if greenhouse gas emissions would stay below the emission levels assumed by RCP8.5.

Overall, this study provides state-of-the-art information on wind power characteristics over the Arctic based on a recent ensemble of regional climate model simulations (Arctic-CORDEX). Of course, reducing uncertainties in projections due to reduced model biases could greatly benefit future investigations, including those improvements in representing wind speeds that may arise from higher horizontal resolution. Improvements in in-situ observational coverage and monitoring of wind speed will help in this regard and are sorely needed. Also, temporal, seasonal, and geographical variations in climatic characteristics (such as sea ice decrease, surface roughness, and scenario changes) may introduce some uncertainty into such projections. Nonetheless, the global long-term transition to renewable energy sources for

environmental sustainability means that the results of this study are vital. Detailed projections of changes in wind speed and WPD are crucial for the development and sustainability of not only wind power systems, but also energy supply that is necessary in order to prevent energy crises. Therefore, the improvement in climate models (ranging from improved model physics to better representation of local conditions in the Arctic) may allow a more robust projection of wind energy potential.

## Declaration of Competing Interest

The authors declare that they have no known competing financial interests or personal relationships that could have appeared to influence the work reported in this paper.

## Data Availability

Data will be made available on request.

## Acknowledgements

The development and implementation of the bias correction scheme were supported by the Russian Science Foundation (RSF № 21-17-00012). WPD analysis was supported by the Russian Science Foundation (RSF № 23-47-00104). Wind speed analysis was supported by the Russian Science Foundation (RSF № 19-17-00240). The analysis of predicted changes of WPD was supported by Russian Ministry of Science and Higher Education (Agreement №. 075-15-2021-577) and partly supported by Russian Center of Scientific Information №. 20-55-14003. Dmitry Sein was supported by the Germany-Sino Joint Project (ACE, No. 2019YFE0125000 and 01LP2004A) and the SIO RAS State Assignment (№ FMWE-2021-0014). AR and HM were partly supported by the European Union’s Horizon 2020 research and innovation framework programme under Grant agreement no. 101003590 (PolarRES) and 869471 (CHARTER). WZ was supported by the grants from Swedish Research Council VR (2020–05338) and Swedish National Space Agency (209/19). This study is a contribution to the strategic research areas Modeling the Regional and Global Earth System (MERGE) at Lund University.

## Appendix A. Supporting information

Supplementary data associated with this article can be found in the online version at [doi:10.1016/j.ancene.2023.100402](https://doi.org/10.1016/j.ancene.2023.100402).

## References

- Akperov, M., Semenov, V.A., Mokhov, I.I., Dorn, W., Rinke, A., 2020. Impact of Atlantic water inflow on winter cyclone activity in the Barents Sea: insights from coupled regional climate model simulations. In: *Environmental Research Letters*, 15. IOP Publishing, p. 24009. <https://doi.org/10.1088/1748-9326/ab6399>.
- Akperov, M., Zhang, W., Miller, P.A., Mokhov, I.I., Semenov, V.A., Matthes, H., Smith, B., Rinke, A., 2021. Responses of Arctic cyclones to biogeophysical feedbacks under future warming scenarios in a regional Earth system model. In: *Environmental Research Letters*, 16. IOP Publishing, p. 64076. <https://doi.org/10.1088/1748-9326/ac0566>.
- Akperov, M., Rinke, A., Mokhov, I.I., Semenov, V.A., Parfenova, M.R., Matthes, H., Adakudlu, M., Boberg, F., Christensen, J.H., Dembitskaya, M.A., Dethloff, K., Fettweis, X., Gutjahr, O., Heinemann, G., Koenigk, T., Koldunov, N.V., Laprise, R., Mottram, R., Nikiéma, O., Sein, D., Sobolowski, S., Winger, K., Zhang, W., 2019. Future projections of cyclone activity in the Arctic for the 21st century from regional climate models (Arctic-CORDEX). *Glob. Planet. Change* 182. <https://doi.org/10.1016/j.gloplacha.2019.103005>.
- Akperov, M., Rinke, A., Mokhov, I.I., Matthes, H., Semenov, V.A., Adakudlu, M., Cassano, J., Christensen, J.H., Dembitskaya, M.A., Dethloff, K., Fettweis, X., Glisan, J., Gutjahr, O., Heinemann, G., Koenigk, T., Koldunov, N.V., Laprise, R., Mottram, R., Nikiéma, O., Scinocca, J.F., Sein, D., Sobolowski, S., Winger, K., Zhang, W., 2018. Cyclone activity in the arctic from an ensemble of regional climate models (Arctic CORDEX). *J. Geophys. Res.: Atmospheres* 123 (5), 2537–2554. <https://doi.org/10.1002/2017JD027703>.
- Akperov, M.G., Eliseev, A.V., Mokhov, I.I., Semenov, V.A., Parfenova, M.R., Koenigk, T., 2022. Wind energy potential in the Arctic and Subarctic regions and its projected change in the 21st century based on regional climate model simulations. *Rus. Meteorol. Hydrol.* 47 (6), 428–436.

- Arora, V.K., Scinocca, J.F., Boer, G.J., Christian, J.R., Denman, K.L., Flato, G.M., Kharin, V.V., Lee, W.G., Merryfield, W.J., 2011. Carbon emission limits required to satisfy future representative concentration pathways of greenhouse gases. In: *Geophysical Research Letters*, 38. John Wiley & Sons, Ltd., <https://doi.org/10.1029/2010GL046270>.
- Benjamini, Y., Hochberg, Y., 1995. Controlling the false discovery rate: a practical and powerful approach to multiple testing. *J. R. Stat. Soc.: Ser. B (Methodol.)* 57 (1), 289–300.
- Bentsen, M., Bethke, I., Debernard, J.B., Iversen, T., Kirkevåg, A., Selund, Ø., Drange, H., Roelandt, C., Seierstad, I.A., Hoose, C., Kristjánsson, J.E., 2013. The Norwegian Earth System Model, NorESM1-M – part 1: description and basic evaluation of the physical climate. *Geosci. Model Dev.* 6 (3), 687–720. <https://doi.org/10.5194/gmd-6-687-2013>.
- Berg, P., Döscher, R., Koenigk, T., 2013. Impacts of using spectral nudging on regional climate model RCA4 simulations of the Arctic. *Geosci. Model Dev.* 6 (3), 849–859. <https://doi.org/10.5194/gmd-6-849-2013>.
- Carvalho, D., Rocha, A., Costoya, X., deCastro, M., Gómez-Gesteira, M., 2021. Wind energy resource over Europe under CMIP6 future climate projections: what changes from CMIP5 to CMIP6. *Renew. Sustain. Energy Rev.* 151 (July) <https://doi.org/10.1016/j.rser.2021.111594>.
- Christensen, J.H., Christensen, O.B., 2007. A summary of the PRUDENCE model projections of changes in European climate by the end of this century. *Clim. Change* 81 (SUPPL. 1), 7–30. <https://doi.org/10.1007/s10584-006-9210-7>.
- Collins, M., Knutti, R., Arblaster, J., Dufresne, J.-L., Fichet, T., Friedlingstein, P., Gao, X., Gutowski, W.J., Johns, T., Krinner, G., Shongwe, M., Tebaldi, C., Weaver, A. J., Wehner, M.F., Allen, M.R., Andrews, T., Beyerle, U., Bitz, C.M., Bony, S., Booth, B. B.B., 2013. Long-term Climate Change: Projections, Commitments and Irreversibility. In: Stocker, T.F., Qin, D., Plattner, G.-K., Tignor, M.M.B., Allen, S.K., Boschung, J., Nauels, A., Xia, Y., Bex, V., Midgley, P.M. (Eds.), *Climate Change 2013 - The Physical Science Basis*. Cambridge University Press, United Kingdom, pp. 1029–1136.
- Docquier, D., Koenigk, T., 2021. Observation-based selection of climate models projects Arctic ice-free summers around 2035. *Commun. Earth Environ.* 2 (1), 144 <https://doi.org/10.1038/s43247-021-00214-7>.
- Dörenkämper, M., Olsen, B.T., Witha, B., Hahmann, A.N., Davis, N.N., Barcons, J., Ezber, Y., Garcíia-Bustamante, E., González-Rouco, J.F., Navarro, J., Sastre-Marugán, M., Sile, T., Trei, W., Žagar, M., Badger, J., Gottschall, J., Sanz Rodrigo, J., Mann, J., 2020. The making of the new European wind atlas – part 2: production and evaluation. *Geosci. Model Dev.* 13 (10), 5079–5102. <https://doi.org/10.5194/gmd-13-5079-2020>.
- Eliseev, A.V., Mokhov, I.I., 2011. Uncertainty of climate response to natural and anthropogenic forcings due to different land use scenarios. *Adv. Atmos. Sci.* 28 (5), 1215–1232. <https://doi.org/10.1007/s00376-010-0054-8>.
- Eliseev, A.V., Semenov, V.A., 2016. Arctic climate changes in the 21st century: ensemble model estimates accounting for realism in present-day climate simulation. *Dokl. Earth Sci.* 471 (1), 1183–1187. <https://doi.org/10.1134/S1028334x16110131>.
- Emeis S. 2005. How Well Does a Power Law Fit to a Diabatic Boundary-Layer Wind Profile?
- Emeis S. 2013. Wind energy meteorology: atmospheric physics for wind power generation.
- Fabiano, F., Christensen, H.M., Strommen, K., Athanasiadis, P., Baker, A., Schiemann, R., Corti, S., 2020. Euro-Atlantic weather Regimes in the PRIMAVERA coupled climate simulations: impact of resolution and mean state biases on model performance. In: *Climate Dynamics*, 54. Springer Berlin Heidelberg, pp. 5031–5048. <https://doi.org/10.1007/s00382-020-05271-w>.
- Fettweis, X., Box, J.E., Agosta, C., Amory, C., Kittel, C., Lang, C., van As, D., Machugh, H., Gallée, H., 2017. Reconstructions of the 1900–2015 Greenland ice sheet surface mass balance using the regional climate MAR model. *Cryosphere* 11 (2), 1015–1033. <https://doi.org/10.5194/10.1015-2017>.
- Giorgetta, M.A., Jungclaus, J., Reick, C.H., Legutke, S., Bader, J., Böttinger, M., Brovkin, V., Crueger, T., Esch, M., Fieg, K., Glushak, K., Gayler, V., Haak, H., Hollweg, H.-D., Ilyina, T., Kinne, S., Kornbluh, L., Matei, D., Mauritsen, T., Mikolajewicz, U., Mueller, W., Notz, D., Pithan, F., Raddatz, T., Rast, S., Redler, R., Roeckner, E., Schmidt, H., Schnur, R., Segschneider, J., Six, K.D., Stockhause, M., Timmreck, C., Wegner, J., Widmann, H., Wieners, K.-H., Claussen, M., Marotzke, J., Stevens, B., 2013. Climate and carbon cycle changes from 1850 to 2100 in MPI-ESM simulations for the Coupled Model Intercomparison Project phase 5. *J. Adv. Model. Earth Syst.* 5 (3), 572–597. <https://doi.org/10.1002/jame.20038>.
- Gruber, K., Regner, P., Wehrle, S., Zeyringer, M., Schmidt, J., 2022. Towards global validation of wind power simulations: A multi-country assessment of wind power simulation from MERRA-2 and ERA-5 reanalyses bias-corrected with the global wind atlas. *Energy* 238, 121520. <https://doi.org/10.1016/j.energy.2021.121520>.
- Gutjahr, O., Heinemann, G., 2018. A model-based comparison of extreme winds in the Arctic and around Greenland. *Int. J. Climatol.* 38 (14), 5272–5292. <https://doi.org/10.1002/joc.5729>.
- Haas, R., Pinto, J.G., Born, K., 2014a. Can dynamically downscaled windstorm footprints be improved by observations through a probabilistic approach? *J. Geophys. Res.* 119 (2), 713–725. <https://doi.org/10.1002/2013JD020882>.
- Haas, R., Pinto, J.G., Born, K., 2014b. Can dynamically downscaled windstorm footprints be improved by observations through a probabilistic approach?. In: *Journal of Geophysical Research: Atmospheres*, 119 John Wiley & Sons, Ltd, pp. 713–725. <https://doi.org/10.1002/2013JD020882>.
- Hazeleger, W., Severijns, C., Semmler, T., Ștefănescu, S., Yang, S., Wang, X., Wyser, K., Dutra, E., Baldasano, J.M., Bintanja, R., Bougeault, P., Caballero, R., Ekman, A.M.L., Christensen, J.H., Van Den Hurk, B., Jimenez, P., Jones, C., Kållberg, P., Koenigk, T., McGrath, R., Miranda, P., Van Noije, T., Palmer, T., Parodi, J.A., Schmith, T., Selten, F., Storelmo, T., Sterl, A., Tapamo, H., Vancoppenolle, M., Viterbo, P., Willén, U., 2012. EC-Earth: a seamless Earth-system prediction approach in action. *Clim. Dyn.* 39 (11), 2609–2610. <https://doi.org/10.1175/2010BAMS2877.1>.
- Heinemann, G., Drüe, C., Makstas, A., 2022. A Three-Year Climatology of the Wind Field Structure at Cape Baranova (Severnaya Zemlya, Siberia) from SODAR Observations and High-Resolution Regional Climate Model Simulations during YOPP. *Atmosphere* 13 (6). <https://doi.org/10.3390/atmos13060957>.
- Hersbach, H., Bell, B., Berrisford, P., Hirahara, S., Horányi, A., Muñoz-Sabater, J., Nicolas, J., Peubey, C., Radu, R., Schepers, D., Simmons, A., Soci, C., Abdalla, S., Abellan, X., Balsamo, G., Bechtold, P., Biavati, G., Bidlot, J., Bonavita, M., De Chiara, G., Dahlgren, P., Dee, D., Diamantakis, M., Dragani, R., Flemming, J., Forbes, R., Fuentes, M., Geer, A., Haimberger, L., Healy, S., Hogan, R.J., Hólm, E., Janisková, M., Keeley, S., Laloyaux, P., Lopez, P., Lupu, C., Radnoti, G., de Rosnay, P., Rozum, I., Vamborg, F., Villaume, S., Thépaut, J.-N., 2020. The ERA5 global reanalysis. In: *Quarterly Journal of the Royal Meteorological Society*, 146. John Wiley & Sons, Ltd, pp. 1999–2049. <https://doi.org/10.1002/qj.3803>.
- Hosking, J.S., MacLeod, D., Phillips, T., Holmes, C.R., Watson, P., Shuckburgh, E.F., Mitchell, D., 2018. Changes in European wind energy generation potential within a 1.5°C warmer world. In: *Environmental Research Letters*, 13. IOP Publishing, p. 54032. <https://doi.org/10.1088/1748-9326/aabf78>.
- Hueging, H., Haas, R., Born, K., Jacob, D., Pinto, J.G., 2013. Regional changes in wind energy potential over Europe using regional climate model ensemble projections. *J. Appl. Meteorol. Climatol.* 52 (4), 903–917. <https://doi.org/10.1175/JAMC-D-12-086.1>.
- Jakobson, L., Vihma, T., Jakobson, E., 2019. Relationships between sea ice concentration and wind speed over the Arctic Ocean during 1979–2015. *J. Clim.* 32 (22), 7783–7796. <https://doi.org/10.1175/JCLI-D-19-0271.1>.
- Jansen, E., Christensen, J.H., Dokken, T., Nisancioglu, K.H., Vinther, B.M., Capron, E., Guo, C., Jensen, M.F., Langen, P.L., Pedersen, R.A., Yang, S., Bentsen, M., Kjær, H.A., Sadatzki, H., Sessford, E., Stendel, M., 2020. Past perspectives on the present era of abrupt Arctic climate change. *Nat. Clim. Change* 10 (8), 714–721. <https://doi.org/10.1038/s41558-020-0860-7>.
- Jung, C., Schindler, D., 2022. A review of recent studies on wind resource projections under climate change. *Renew. Sustain. Energy Rev.* 165, 112596 <https://doi.org/10.1016/j.rser.2022.112596>.
- Khon, V.C., Mokhov, I.I., Semenov, V.A., 2017. Transit navigation through Northern Sea Route from satellite data and CMIP5 simulations. In: *Environmental Research Letters*, 12. IOP Publishing, p. 24010. <https://doi.org/10.1088/1748-9326/aa5841>.
- Kibanova, O.V., Eliseev, A.V., Mokhov, I.I., Khon, V.C., 2018. Variations in the duration of the navigation period along The Northern Sea Route in the 21st century based on simulations with an ensemble of climatic models: bayesian estimates. *Dokl. Earth Sci.* 481 (1), 907–911. <https://doi.org/10.1134/S1028334x18070073>.
- Klaus, D., Dethloff, K., Dorn, W., Rinke, A., Wu, D.L., 2016. New insight of Arctic cloud parameterization from regional climate model simulations, satellite-based, and drifting station data. *Geophys. Res. Lett.* 43 (10), 5450–5459. <https://doi.org/10.1002/2015GL067530>.
- Koenigk, T., Berg, P., Döscher, R., 2015. Arctic climate change in an ensemble of regional CORDEX simulations. *Polar Res.* 34 (2015), 1–2019 <https://doi.org/10.3402/polar.v34.24603>.
- Koenigk, T., Brodeau, L., Graverson, R.G., Karlsson, J., Svensson, G., Tjernström, M., Willén, U., Wyser, K., 2013. Arctic climate change in 21st century CMIP5 simulations with EC-Earth. *Clim. Dyn.* 40 (11), 2719–2743. <https://doi.org/10.1007/s00382-012-1505-y>.
- Kryl'tsov, S., Solov'ev, S., 2019. Efficient wind energy generation within Arctic latitudes. *E3S Web Conf.* 140, 1–4. <https://doi.org/10.1051/e3sconf/201914011005>.
- Lambin, C., Fettweis, X., Kittel, C., Fonder, M., Ernst, D., 2023. Assessment of future wind speed and wind power changes over South Greenland using the Modèle Atmosphérique Regional regional climate model. *Int. J. Climatol.* 43 (1), 558–574. <https://doi.org/10.1002/joc.7795>.
- Laurila, T.K., Sinclair, V.A., Gregor, H., 2021. Climatology, variability, and trends in near-surface wind speeds over the North Atlantic and Europe during 1979–2018 based on ERA5. In: *International Journal of Climatology*, 41. John Wiley & Sons, Ltd, pp. 2253–2278. <https://doi.org/10.1002/joc.6957>.
- Li, D., Feng, J., Xu, Z., Yin, B., Shi, H., Qi, J., 2019a. Statistical bias correction for simulated wind speeds over CORDEX-east asia. *Earth Space Sci.* 6 (2), 200–211. <https://doi.org/10.1029/2018EA000493>.
- Li, D., Feng, J., Xu, Z., Yin, B., Shi, H., Qi, J., 2019b. Statistical bias correction for simulated wind speeds over CORDEX-East Asia. In: *Earth and Space Science*, 6. John Wiley & Sons Ltd, pp. 200–211. <https://doi.org/10.1029/2018EA000493>.
- Li, D., Feng, J., Dosio, A., Qi, J., Xu, Z., Yin, B., 2020. Historical evaluation and future projections of 100-m wind energy potentials over CORDEX-East Asia. *J. Geophys. Res.: Atmospheres* 125 (15), 1–18. <https://doi.org/10.1029/2020JD032874>.
- Lucas-Picher, P., Wulff-Nielsen, M., Christensen, J.H., Aðalgeirsdóttir, G., Mottram, R., Simonsen, S.B., 2012. Very high resolution regional climate model simulations over Greenland: Identifying added value. *J. Geophys. Res.: Atmospheres* 117 (D2), n/a/n/a. <https://doi.org/10.1029/2011JD016267>.
- Lüpfkes, C., Gryanik, V.M., Rösel, A., Birnbaum, G., Kaleschke, L., 2013. Effect of sea ice morphology during Arctic summer on atmospheric drag coefficients used in climate models. *Geophys. Res. Lett.* 40 (2), 446–451. <https://doi.org/10.1002/grl.50081>.
- Mann, H.B., Whitney, D.R., 1947. On a test of whether one of two random variables is stochastically larger than the other. *Ann. Math. Stat.* 50–60. <https://doi.org/10.1214/aoms/1177730491>.
- Martynov, A., Laprise, R., Sushama, L., Winger, K., Šeparović, L., Dugas, B., 2013. Reanalysis-driven climate simulation over CORDEX North America domain using the

- Canadian Regional Climate Model, version 5: model performance evaluation. *Clim. Dyn.* 41 (11–12), 2973–3005. <https://doi.org/10.1007/s00382-013-1778-9>.
- Massonnet, F., Fichet, T., Goosse, H., Bitz, C.M., Philippon-Berthier, G., Holland, M.M., Barriat, P.-Y., 2012. Constraining projections of summer Arctic sea ice. *Cryosphere* 6 (6), 1383–1394. <https://doi.org/10.5194/tc-6-1383-2012>.
- Mba, W.P., Longandjo, G.N.T., Moufouma-Okia, W., Bell, J.P., James, R., Vondou, D.A., Haensler, A., Fotso-Nguemo, T.C., Guenang, G.M., Tchotchou, A.L.D., Kamsu-Tamo, P.H., Takong, R.R., Nikulin, G., Lennard, C.J., Dosio, A., 2018. Consequences of 1.5 °C and 2 °C global warming levels for temperature and precipitation changes over Central Africa. *Environ. Res. Lett.* 13 (5) <https://doi.org/10.1088/1748-9326/aab048>.
- McKenna, R., Ostman, P., Fichtner, W., 2016. Key challenges and prospects for large wind turbines. *Renewable and Sustainable Energy Reviews*. Elsevier Ltd, pp. 1212–1221.
- Minola, L., Zhang, F., Azorin-Molina, C., Pirooz, A.A.S., Flay, R.G.J., Hersbach, H., Chen, D., 2020. Near-surface mean and gust wind speeds in ERA5 across Sweden: towards an improved gust parametrization. *Clim. Dyn.* 55 (3), 887–907. <https://doi.org/10.1007/s00382-020-05302-6>.
- Mioduszewski, J., Vavrus, S., Wang, M., 2018. Diminishing Arctic Sea Ice Promotes Stronger Surface Winds. In: *Journal of Climate*, 31. American Meteorological Society, Boston MA, USA, pp. 8101–8119. <https://doi.org/10.1175/JCLI-D-18-0109.1>.
- Moemken, J., Reyers, M., Feldmann, H., Pinto, J.G., 2018. Future Changes of Wind Speed and Wind Energy Potentials in EURO-CORDEX Ensemble Simulations. *J. Geophys. Res.: Atmosph.* 123 (12), 6373–6389. <https://doi.org/10.1029/2018JD028473>.
- Mokhov, I.I., Parfenova, M.R., 2021. Relationship of the extent of Antarctic and Arctic sea ice with temperature changes, 1979–2020 // *Dokl. Earth Sci. V. 496 (N<sup>o</sup> 1)*, 66–71.
- Nikolaev V. G., Ganaga S. V. and Kudryashov Yu. I., National Cadastre of Wind Energy Resources of Russia and Methodological Basis for Their Determination (Atmograf, Moscow, 2008) [in Russian].
- Nikulin, G., Lennard, C., Dosio, A., Kjellström, E., Chen, Y., Hansler, A., Kupiainen, M., Laprise, R., Mariotti, L., Maule, C.F., Van Meijgaard, E., Panitz, H.J., Scinocca, J.F., Somot, S., 2018. The effects of 1.5 and 2 degrees of global warming on Africa in the CORDEX ensemble. *Environ. Res. Lett.* 13 (6) <https://doi.org/10.1088/1748-9326/aab1b1>.
- Olauson, J., 2018. ERA5: The new champion of wind power modelling? *Renew. Energy* 126, 322–331. <https://doi.org/10.1016/j.renene.2018.03.056>.
- Parfenova, M.R., Eliseev, A.V., Mokhov, I.I., 2021. Changes in the duration of the navigation period in Arctic seas along the Northern Sea Route in the twenty-first century: Bayesian estimates based on calculations with the ensemble of climate models. *Dokl. Earth Sci. V. 507 (1)*, 952–958.
- Pearson, R.G., Phillips, S.J., Lorant, M.M., Beck, P.S.A., Damoulas, T., Knight, S.J., Goetz, S.J., 2013. Shifts in Arctic vegetation and associated feedbacks under climate change. *Nat. Clim. Change* 3 (7), 673–677. <https://doi.org/10.1038/nclimate1858>.
- Pryor, S.C., Schoof, J.T., Barthelmie, R.J., 2005. Empirical downscaling of wind speed probability distributions. *J. Geophys. Res.: Atmospheres*. John Wiley Sons, Ltd 110 (D19). <https://doi.org/10.1029/2005JD005899>.
- Ramon, J., Lledó, L., Torralba, V., Soret, A., Doblas-Reyes, F.J., 2019. What global reanalysis best represents near-surface winds?. In: *Quarterly Journal of the Royal Meteorological Society*, 145 John Wiley & Sons, Ltd, pp. 3236–3251. <https://doi.org/10.1002/qj.3616>.
- Rantanen, M., Karpechko, A.Y., Lipponen, A., Nordling, K., Hyvärinen, O., Ruosteenoja, K., Vihma, T., Laaksonen, A., 2022. The Arctic has warmed nearly four times faster than the globe since 1979. *Commun. Earth Environ.* 3 (1), 168 <https://doi.org/10.1038/s43247-022-00498-3>.
- Rapella, L., Faranda, D., Gaetani, M., Drobninski, P., Ginesta, M., 2023. Climate change on extreme winds already affects off-shore wind power availability in Europe. *Environ. Res. Lett.* 18 (3) <https://doi.org/10.1088/1748-9326/acdbb2>.
- Rasmussen, E.A., Turner, J., 2003. *Polar lows: mesoscale weather systems in the polar regions*. Cambridge University Press, p. 612.
- Semenov, V.A., Latif, M., 2015. Nonlinear winter atmospheric circulation response to Arctic sea ice concentration anomalies for different periods during 1966 – 2012 Nonlinear winter atmospheric circulation response to Arctic sea ice concentration anomalies for different periods during 1. IOP Publishing. <https://doi.org/10.1088/1748-9326/10/5/054020>.
- Šeparović, L., Alexandru, A., Laprise, R., Martynov, A., Sushama, L., Winger, K., Tete, K., Valin, M., 2013. Present climate and climate change over North America as simulated by the fifth-generation Canadian regional climate model. *Clim. Dyn.* 41 (11–12), 3167–3201. <https://doi.org/10.1007/s00382-013-1737-5>.
- Smith, B., Samuelsson, P., Wramneby, A., Rummukainen, M., 2011. A model of the coupled dynamics of climate, vegetation and terrestrial ecosystem biogeochemistry for regional applications. *Tellus, Ser. A: Dyn. Meteorol. Oceanogr.* 63 (1), 87–106. <https://doi.org/10.1111/j.1600-0870.2010.00477.x>.
- Soares, P.M.M., Lima, D.C.A., Nogueira, M., 2020. Global offshore wind energy resources using the new ERA5 reanalysis. In: *Environmental Research Letters*, 15. {IOP} Publishing, p. 1040a2. <https://doi.org/10.1088/1748-9326/abb10d>.
- Sommerfeld, A., Nikiema, O., Rinke, A., Dethloff, K., Laprise, R., 2015. Arctic budget study of intermember variability using HIRHAM5 ensemble simulations. *J. Geophys. Res.: Atmospheres* 120 (18), 9390–9407. <https://doi.org/10.1002/2015JD023153>.
- T. Vihma *Eff. Arct. Sea Ice Decline Weather Clim.: A Rev. Surv. Geophys.* 2014.
- Takhsha, M., Nikiema, O., Lucas-Picher, P., Laprise, R., Hernández-Díaz, L., Winger, K., 2017. Dynamical downscaling with the fifth-generation Canadian regional climate model (CRCM5) over the CORDEX Arctic domain: effect of large-scale spectral nudging and of empirical correction of sea-surface temperature. In: *Climate Dynamics*, 0. Springer Berlin Heidelberg, pp. 1–26. <https://doi.org/10.1007/s00382-017-3912-6>.
- Taylor, K.E., Stouffer, R.J., Meehl, G.A., 2012. An overview of CMIP5 and the experiment design. *Bull. Am. Meteorol. Soc.* 93 (4), 485–498. <https://doi.org/10.1175/BAMS-D-11-00094.1>.
- Tobin, I., Vautard, R., Balog, I., Bréon, F.-M., Jerez, S., Ruti, P., Thais, F., Vrac, M., Yiou, P., 2015. Assessing climate change impacts on European wind energy from ENSEMBLES high-resolution climate projections. *Clim. Change* 128 (1), 99–112. <https://doi.org/10.1007/s10584-014-1291-0>.
- Tuononen, M., Sinclair, V.A., Vihma, T., 2015. A climatology of low-level jets in the mid-latitudes and polar regions of the Northern Hemisphere. *Atmos. Sci. Lett.* 16 (4), 492–499. <https://doi.org/10.1002/asl.587>.
- Vavrus, S.J., Alkama, R., 2021. Future trends of arctic surface wind speeds and their relationship with sea ice in CMIP5 climate model simulations. *Climate Dynamics*. Springer, Berlin Heidelberg, 0123456789. <https://doi.org/10.1007/s00382-021-06071-6>.
- Wilks, D., 2016. The stippling shows statistically significant grid points: how research results are routinely overstated and overinterpreted, and what to do about it. *Bull. Am. Meteorol. Soc.* 97 (12), 2263–2273.
- Zhang, W., Jansson, C., Miller, P.A., Smith, B., Samuelsson, P., 2014. Biogeophysical feedbacks enhance the Arctic terrestrial carbon sink in regional Earth system dynamics. *Biogeosciences* 11 (19), 5503–5519. <https://doi.org/10.5194/bg-11-5503-2014>.
- Zhang, W., Miller, P.A., Jansson, C., Samuelsson, P., Mao, J., Smith, B., 2018. Self-amplifying feedbacks accelerate greening and warming of the arctic. *Geophys. Res. Lett.* 45 (14), 7102–7111. <https://doi.org/10.1029/2018GL077830>.